Soft Matter

PAPER

View Article Online
View Journal | View Issue

Cite this: *Soft Matter*, 2016, 12, 6771

Adsorption of flexible polyelectrolytes on charged surfaces

A. V. Subbotin[a] and A. N. Semenov*[b]

Received 17th May 2016,
Accepted 15th July 2016

DOI: 10.1039/c6sm01140c

www.rsc.org/softmatter

Adsorption of weakly charged polyelectrolyte (PE) chains from dilute solution on an oppositely charged surface is studied using the self-consistent mean-field approach. The structure of the adsorbed polymer layer and its excess charge are analyzed in the most important asymptotic and intermediate regimes both analytically and numerically. Different regimes of surface charge compensation by PE chains including partial and full charge inversion are identified and discussed in terms of physical parameters like the magnitude of specific short-range interactions of PE segments with the surface, solvent quality and ionic strength. The effect of excluded-volume monomer interactions is considered quantitatively both in the marginally good and poor solvent regimes.

1 Introduction

Let us consider a dilute solution of polyelectrolyte (PE) chains. In the presence of an oppositely charged surface the PE chains tend to form an adsorbed layer on it. Polyelectrolyte adsorption is an important phenomenon widely used for practical purposes including the stabilization of colloidal dispersions in numerous biological and industrial applications.[1] The adsorbed layers are generically involved in many technologically important PE systems, including polyelectrolyte multilayers, vesicles, templates, *etc.* Understanding the structure of PE layers and the physics behind it is a challenging general problem.

It is known that upon adsorption the total charge of the surface plus the adsorbed polymer can be opposite to the initial bare surface charge.[2,3,5,7–9] This phenomenon, known as charge inversion, is important fundamentally and it seems to provide the driving force for the alternate adsorption of positively and negatively charged polymers, leading to the so-called PE multilayer formation.[3,11,12] While the significance of this purely electrostatic driving force has been questioned since other more specific forces can (and often do) contribute to multilayer stability,[10] the very fact that multilayers are typically and easily assembled by charged polymers points to the crucial role of electrostatic effects including the charge inversion phenomenon.

Adsorption of PEs on a charged surface was studied theoretically in ref. 6 for the case of constant surface potential and strongly repulsive short-range interactions of uncharged polymer segments with the surface (nonadsorbing surface). The problem was studied both numerically and by scaling analysis. The predictions[6] concerning the polymer layer thickness and surface excess are generally in agreement with our results (see Discussion, Section 4.3). However, specifically the excess surface charge due to the adsorbed PE was not considered in ref. 6. The latter quantity was analysed by Joanny[7] who developed a theory of polyelectrolyte adsorption from dilute solution on an oppositely charged surface based on a mean-field model rather similar to that adopted in ref. 6. The study[7] was mainly focused on the ideal polymer regimes with insignificant non-Coulombic interactions between polymer segments, discussing briefly the effects of their 3-body excluded-volume interactions and non-electrostatic monomer/surface interactions; the effects of 2-body monomer interactions have not been discussed there. One aim of the present paper is to generalize the theory[7] and to analyse the solvent quality and surface interaction effects in more detail. Another aim is to provide a more complete and quantitative analytical description of the charge inversion effect in the asymptotic regimes of low and high ionic strength and in other regimes. It was found[7] that the excess charge of the adsorbed layer, σ_{ex}, is inversely proportional to the Debye length r_D at low salt concentration. However, this general relationship has not been fully justified and has been missing a proper prefactor. These gaps are also filled in our study.

PE adsorption and charge inversion phenomena have been studied theoretically more recently in ref. 4, 8 and 9. They used a mean-field approach similar to that of ref. 7, and altogether they generalized the theory to include the monomer and surface interactions. So why do we address the problem again? The point is that the results of ref. 8 and 9 seem to contradict each other: in ref. 8 a full charge inversion was not found (and it was concluded that multilayer formation must rely on non-electrostatic effects), while the regimes of full or even stronger overcharging are predicted in ref. 9. In both cases the results have been

[a] *A. V. Topchiev Institute of Petrochemical Synthesis, Russian Academy of Sciences, Leninskii prosp. 29, Moscow, 119991, Russia. E-mail: subbotin@ips.ac.ru*
[b] *Institut Charles Sadron, CNRS – UPR 22, Université de Strasbourg, 23 rue du Loess, 67034 Strasbourg Cedex 2, France. E-mail: semenov@unistra.fr*

obtained mostly numerically: the analytical parts of these studies are more auxiliary and are not entirely satisfactory in our opinion (it was stated[9] that their analytical approach involves 'problematic' approximations). To resolve the issue we considered the same simple mean-field model in a more analytical fashion which allows us to built a more complete picture of possible adsorption regimes and to quantitatively find the degree of overcharging (or undercharging) depending on the conditions. To facilitate this task we identified the basic reduced parameters characterizing the system. This allows us to systematically describe all the regimes in terms of a minimal set of essential parameters. For example, in the case of ideal polymer backbones and purely repulsive surfaces the adsorbed layer structure essentially depends on only one parameter, the reduced ionic strength ν.

The model, the basic mean-field equations, and the results of their numerical study highlighting the effects of ionic strength, polymer/surface and excluded-volume interactions on PE adsorption are presented in the next 2 sections. The main results are discussed in detail in Section 4 and the main conclusions are outlined in the last section.

2 Model and basic equations

In this paper we consider adsorbed layers of long weakly charged flexible PE chains (with a low fraction $f \ll 1$ of positively charged units† and a large polymerization index $N \gg 1/f$) in the regime of moderate polymer density in the layer (corresponding to semidilute solution). In this regime the excluded-volume interactions between polymer segments can be described in terms of virial coefficients B and C defining the relevant free energy density

$$F_{ex} \simeq k_B T\left(\frac{B}{2}n^2 + \frac{C}{6}n^3\right)$$

where n is the concentration of monomer residues, k_B is the Boltzmann constant, and T is the temperature. The corresponding chemical potential at distance z to the surface,

$$\mu_{ex} = \frac{\partial F_{ex}}{\partial n} = k_B T\left(Bn + Cn^2/2\right), \qquad (1)$$

depends on the local concentration $n = n(z)$. In what follows we assume the limiting case of dilute bulk PE solution (zero bulk concentration):

$$n(z) \to 0 \text{ at } z \to \infty.$$

The surface is negatively charged with density $-e\sigma$, where σ is the number of $-e$ charges per unit area. The volume density of charge is $\rho = e(fn + c_+ - c_-)$, where c_+ and c_- are concentrations of small ions (in particular due to the added salt). In the mean-field approximation (adopted throughout the paper)

$$c_\pm = c_b \exp(\mp\Phi) \qquad (2)$$

where $\Phi = e\varphi/(k_B T)$, $\varphi = \varphi(z)$ is the electrostatic potential and c_b is the bulk concentration of anions (ionic strength). It is assumed that the surface charge is not too high, $|\Phi| \ll 1$, so the potential $\Phi(z)$ obeys the Poisson equation in the Debye–Hückel (DH) approximation

$$\frac{d^2\Phi}{dz^2} = r_D^{-2}\Phi - f\tilde{\ell}_B n \qquad (3)$$

where $\Phi = \Phi(z)$, $n = n(z)$, and r_D is the Debye length,

$$r_D^{-2} \simeq 2\tilde{\ell}_B c_b$$

($\tilde{\ell}_B = 4\pi\ell_B$, $\ell_B = \dfrac{e^2}{\varepsilon k_B T}$ is the Bjerrum length, and ε is the dielectric constant of the medium). It is assumed that ε does not significantly depend on polymer concentration since the latter is low ($Cn^2 \ll 1$): $\varepsilon \approx$ const.

Turning to the polymer concentration profile $n(z)$ we note that it can be described within the mean-field ground-state dominance approximation[13–16] since PE chains considered here are very long (polymerization index $N \to \infty$) and flexible (with statistical segment a_s):

$$a^2\frac{d^2\psi}{dz^2} = (U - E)\psi \qquad (4)$$

where $a^2 = a_s^2/6$, $\psi = \sqrt{n}$, and

$$U = \mu_{ex}/(k_B T) + f\Phi$$

is the total effective molecular field (in $k_B T$ units). Here E is a constant, the ground-state 'energy' eigenvalue. The validity of the above Edwards equation is hinged on the condition $U(z) \ll 1$ which is true since polymer concentration is low, $Cn^2 \ll 1$, $f \ll 1$, and $\Phi \ll 1$ (see Appendix A). Note that the ground state eigenvalue E is an important free parameter, $E \leq 0$ (see Section 4.2).

Eqn (3) and (4) should be supplemented by the boundary conditions at the wall and at infinity. For the potential $\varphi(z)$ they read

$$\left.\frac{d\varphi}{dz}\right|_{z=0} = \frac{4\pi e\sigma}{\varepsilon}, \quad \varphi|_{z=\infty} = 0. \qquad (5)$$

The boundary condition for the order parameter $\psi(z)$ at the wall is defined by the polymer/surface interactions. We will separate two cases, namely the case of a steric hard wall when the concentration of the polymer is zero on the surface and the boundary conditions are given by

$$\psi|_{z=0} = 0, \quad \psi|_{z=\infty} = 0 \qquad (6)$$

and the case of an adsorbing wall with specific short-range polymer/wall interactions. The surface concentration of monomers is non-zero in the latter case, $\psi|_{z=0} = \psi_0 \neq 0$, and the boundary conditions are:

$$\left.\frac{d\psi}{dz}\right|_{z=0} = \kappa\psi, \quad \psi|_{z=\infty} = 0. \qquad (7)$$

Here the parameter κ depends on the polymer/surface interactions and can be both positive and negative: $\kappa < 0$ means that the wall attracts the polymer segments both electrostatically and by some specific short-range affinity, whereas the overall short-range polymer/wall interactions are repulsive for $\kappa > 0$.

† The positive sign is chosen just to be specific.

Note that the boundary conditions in eqn 6 are the limiting case of eqn 7 for $\kappa \to \infty$.

In the general case the solution of eqn (2)–(7) depends on the eigenvalue E correlating with the amount of the adsorbed polymer. The most stable polymer layer corresponds to the minimum of the free energy F including the conformational, electrostatic, ideal-gas and excluded-volume interaction terms given by (per unit surface area):

$$F = k_B T \int_0^\infty \mathrm{d}z \left[a^2 \left(\frac{\mathrm{d}\psi}{\mathrm{d}z}\right)^2 + \frac{1}{2\tilde{\ell}_B}\left(\frac{\mathrm{d}\Phi}{\mathrm{d}z}\right)^2 + \frac{B}{2}\psi^4 + \frac{C}{6}\psi^6 + f_{id}(c_+, c_-)\right] \tag{8}$$

where $f_{id}(c_+,c_-) = c_+ \ln c_+ + c_- \ln c_- - (\ln c_b + 1)(c_+ + c_-) + 2c_b$ is the reduced ideal-gas free energy density of small ions.

Eqn (2)–(8) can be rewritten in terms of the following non-dimensional variables:

$$x = z/h_0, \quad \tilde{\psi} = \frac{\psi\sqrt{h_0 f}}{\sqrt{\sigma}}, \quad \tilde{\Phi} = \frac{\varepsilon}{4\pi e h_0 \sigma}\varphi$$

$$E = \frac{a^2}{h_0^2}\tilde{E}, \quad \kappa = \frac{\tilde{\kappa}}{h_0}, \quad B = \frac{a^2 f}{h_0 \sigma}\tilde{B}, \quad C = \frac{2a^2 f^2}{\sigma^2}\tilde{C}$$

where

$$h_0 = \left(\frac{a^2}{f\sigma\tilde{\ell}_B}\right)^{1/3}, \quad \tilde{\ell}_B = \frac{4\pi e^2}{\varepsilon k_B T}. \tag{9}$$

Here h_0 is the characteristic thickness of the adsorbed layer identified in ref. 7. The system involves the second length-scale, the Debye length $r_D = \left(2\tilde{\ell}_B c_b\right)^{-1/2}$. The ratio of the two lengths defines the dimensionless ionic strength parameter $\nu = {h_0}^2/{r_D}^2$. Eqn (3) and (4) with boundary conditions (5) and (7) in the dimensionless form read:

$$\frac{\mathrm{d}^2\tilde{\psi}}{\mathrm{d}x^2} = \left(\tilde{\Phi} - \tilde{E} + \tilde{B}\tilde{\psi}^2 + \tilde{C}\tilde{\psi}^4\right)\tilde{\psi}, \quad \left.\frac{\mathrm{d}\tilde{\psi}}{\mathrm{d}x}\right|_{x=0} = \tilde{\kappa}\tilde{\psi}, \quad \tilde{\psi}|_{x=\infty} = 0 \tag{10}$$

$$\frac{\mathrm{d}^2\tilde{\Phi}}{\mathrm{d}x^2} = -\tilde{\psi}^2 + \nu\tilde{\Phi}, \quad \left.\frac{\mathrm{d}\tilde{\Phi}}{\mathrm{d}x}\right|_{x=0} = 1, \quad \tilde{\Phi}|_{x=\infty} = 0. \tag{11}$$

Eqn (11) can be solved in the general way yielding the following integral form

$$\tilde{\Phi}(x) = \frac{1}{2\sqrt{\nu}}\int_0^\infty \mathrm{d}y \tilde{\psi}^2(y)\left[\mathrm{e}^{-\sqrt{\nu}|x-y|} + \mathrm{e}^{-\sqrt{\nu}|x+y|}\right] - \frac{1}{\sqrt{\nu}}\mathrm{e}^{-x\sqrt{\nu}}. \tag{12}$$

The free energy F can be rewritten as

$$F = k_B T h_0 \sigma^2 \tilde{\ell}_B \tilde{F},$$

$$\tilde{F} = \int_0^\infty \mathrm{d}x \left[\left(\frac{\mathrm{d}\tilde{\psi}}{\mathrm{d}x}\right)^2 + \frac{1}{2}\left(\frac{\mathrm{d}\tilde{\Phi}}{\mathrm{d}x}\right)^2 + \frac{\nu}{2}\tilde{\Phi}^2 + \frac{\tilde{B}}{2}\tilde{\psi}^4 + \frac{\tilde{C}}{3}\tilde{\psi}^6\right]. \tag{13}$$

Eqn (10) and (11) are formally equivalent to mechanical equations for a 2-dimensional classical particle (coordinates $\tilde{\psi}$, $\tilde{\Phi}$) with anisotropic mass, $m_\psi = 2$, $m_\Phi = -1$ in the potential $U = (\tilde{E} - \tilde{\Phi})\tilde{\psi}^2 - \frac{\tilde{B}}{2}\tilde{\psi}^4 - \frac{\tilde{C}}{3}\tilde{\psi}^6 + \frac{\nu}{2}\tilde{\Phi}^2$. The 'mechanical energy' conservation law yields the following integral:

$$\left(\frac{\mathrm{d}\tilde{\psi}}{\mathrm{d}x}\right)^2 - \frac{1}{2}\left(\frac{\mathrm{d}\tilde{\Phi}}{\mathrm{d}x}\right)^2 + \frac{\nu}{2}\tilde{\Phi}^2 - \frac{\tilde{B}}{2}\tilde{\psi}^4 - \frac{\tilde{C}}{3}\tilde{\psi}^6 + (\tilde{E} - \tilde{\Phi})\tilde{\psi}^2 = I = \text{const.} \tag{14}$$

Using boundary conditions at $x \to \infty$ and extinction of the derivatives at $x \to \infty$, $\left.\frac{\mathrm{d}\tilde{\psi}}{\mathrm{d}x}\right|_{x=\infty} = 0$, $\left.\frac{\mathrm{d}\tilde{\Phi}}{\mathrm{d}x}\right|_{x=\infty} = 0$, one finds $I = 0$. Using eqn (14) we obtain an additional condition at $x = 0$:

$$\left.\frac{\mathrm{d}\tilde{\psi}}{\mathrm{d}x}\right|_{x=0} = \sqrt{0.5\left(1 - \nu\tilde{\Phi}_0^2\right)} \tag{15}$$

for the steric hard wall ($\psi|_{z=0} = 0$), and

$$\left(\tilde{\Phi}_0 - \tilde{\kappa}^2 - \tilde{E} + \frac{\tilde{B}}{2}\tilde{\psi}_0^2 + \frac{\tilde{C}}{3}\tilde{\psi}_0^4\right)\tilde{\psi}_0^2 + \frac{1}{2}\left(1 - \nu\tilde{\Phi}_0^2\right) = 0 \tag{16}$$

in the general case, where $\tilde{\psi}_0 = \tilde{\psi}(0)$, $\tilde{\Phi}_0 = \tilde{\Phi}(0)$.

In the next two sections we consider the case of dominating electrostatic interactions (*i.e.*, PE chains with negligible B and C interaction parameters).

3 Numerical results

3.1 Repulsive hard wall

We start the analysis of polyelectrolyte layers with the case of a purely repulsive hard wall ($\kappa = \infty$) and no excluded-volume interactions. The system of eqn (10) and (11) is then written as

$$\frac{\mathrm{d}^2\tilde{\psi}}{\mathrm{d}x^2} = (\tilde{\Phi} - \tilde{E})\tilde{\psi}, \quad \tilde{\psi}|_{x=0} = 0, \quad \tilde{\psi}|_{x=\infty} = 0 \tag{17}$$

$$\frac{\mathrm{d}^2\tilde{\Phi}}{\mathrm{d}x^2} = -\tilde{\psi}^2 + \nu\tilde{\Phi}, \quad \left.\frac{\mathrm{d}\tilde{\Phi}}{\mathrm{d}x}\right|_{x=0} = 1, \quad \tilde{\Phi}|_{x=\infty} = 0. \tag{18}$$

This system was solved numerically. We start with the salt free case $\nu = 0$. Since the electrical field at the infinity is zero, the adsorbed polyelectrolyte layer must completely screen the surface charge in this case. The reduced density profiles of charged monomers, $\tilde{n}_+(x) = \tilde{\psi}^2(x)$, and the reduced potential $\tilde{\Phi}(x)$ are shown in Fig. 1. The potential monotonically increases from $\tilde{\Phi}_0 \approx 2.24$ at the wall, and its main change occurs at $x \sim 3$ corresponding to the length scale $z \sim 3h_0$. The adsorbed layer is localized near the wall at the same distance. At larger distances the polymer concentration and electric potential decay exponentially: $\tilde{n}(x) \sim \tilde{\Phi}(x) \sim \mathrm{e}^{-2x\sqrt{\varepsilon}}$ at $x \gg 1$, where $\varepsilon = -\tilde{E}_0 \approx 0.26$ and subscript '0' indicates that $\nu = 0$.

An added salt, $\nu > 0$, screens the electrostatic interaction at $x \gg 1/\sqrt{\nu}$. Obviously, the length scales $x \sim 1$ and $x \sim 1/\sqrt{\nu}$ (that is h_0 and r_D) are well separated for $\nu \ll 1$. The adsorbed

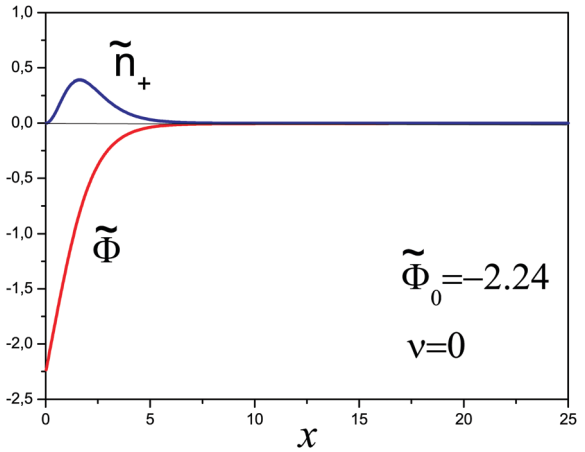

Fig. 1 The reduced concentration of charged monomers $\tilde{n}_+(x)$ and the electric potential $\tilde{\Phi}(x)$.

layer can be characterized by the excess charge σ_{ex} which is the sum of the bare surface charge and the adsorbed layer charge:

$$\sigma_{ex} = \sigma\int_0^\infty \tilde{\psi}^2(x)\mathrm{d}x - \sigma = \sigma\nu\int_0^\infty \tilde{\Phi}(x)\mathrm{d}x. \qquad (19)$$

The total mass of the adsorbed polymer layer and its free energy depend on the parameter $\tilde{E}$. As $\tilde{E}$ is increased the free energy decreases and its minimum is attained at $\tilde{E} = 0$ corresponding to the saturated layer, see Fig. 2. In what follows we consider the saturated layers only, hence we set $\tilde{E} = 0$ for $\nu > 0$. The density profiles of charged monomers and the potential profiles for different values of ν are shown in Fig. 3. In all cases the potential Φ passes through a maximum value. It means that the electric field changes its direction inside the layer. With increasing salt concentration the electrostatic attraction between the wall and the polyelectrolyte chains decreases, so the concentration of the polymer in the layer decreases as well. An adsorbed layer is not formed at all if the amount of salt is high enough: $\nu \geq \nu_c \approx 0.78$.

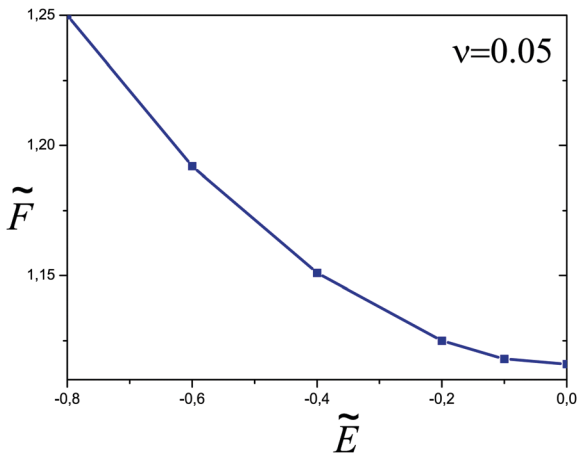

Fig. 2 The free energy of the adsorbed layer as a function of $\tilde{E}$.

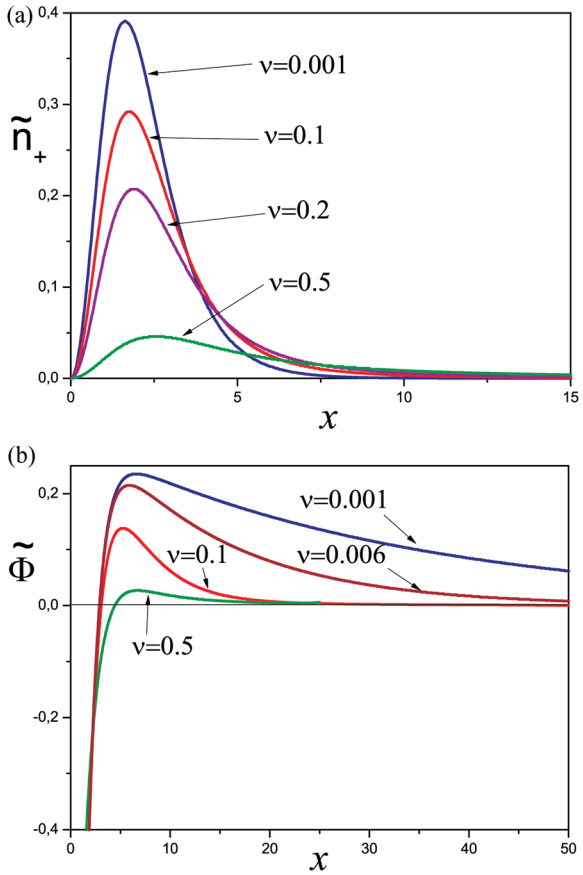

Fig. 3 Properties of saturated layers: concentration profiles of charged monomers (a) and the potential profiles (b) for different $\nu > 0$.

In Fig. 4 we show the plots of the surface potential $\tilde{\Phi}_0$ and the reduced excess surface charge $\tilde{\sigma}_{ex} = \sigma_{ex}/\sigma$ as functions of ν. The surface potential increases monotonically with ionic strength, while the excess surface charge attains the maximum value ($\tilde{\sigma}_{ex} \approx 0.008$) at $\nu \approx 0.004$. The adsorbed polymer layer overcharges the surface (*i.e.*, $\tilde{\sigma}_{ex} > 0$) for $\nu < 0.015$. However, the overcharging effect is very weak and occurs only at low ionic strength (for $r_D \gtrsim 8h_0$).

Based on eqn (18) we established the asymptotic behavior of the potential $\tilde{\Phi}(x)$ at $x \gg 1$ and $\nu \ll 1$ (*cf.* Section 4.2, eqn (28)). It implies that

$$\tilde{\sigma}_{ex} = \nu\int_0^\infty \tilde{\Phi}(x)\mathrm{d}x \simeq 0.26\sqrt{\nu}, \quad \nu \ll 1. \qquad (20)$$

This asymptotic dependence is shown as a dashed line in Fig. 4b.

3.2 Attractive wall

The system of eqn (10) and (11) for the adsorbing wall without volume interactions can be written as

$$\frac{\mathrm{d}^2\tilde{\psi}}{\mathrm{d}x^2} = \tilde{\Phi}\tilde{\psi}, \quad \left.\frac{\mathrm{d}\tilde{\psi}}{\mathrm{d}x}\right|_{x=0} = \tilde{\kappa}\tilde{\psi}, \quad \tilde{\psi}|_{x=\infty} = 0 \qquad (21)$$

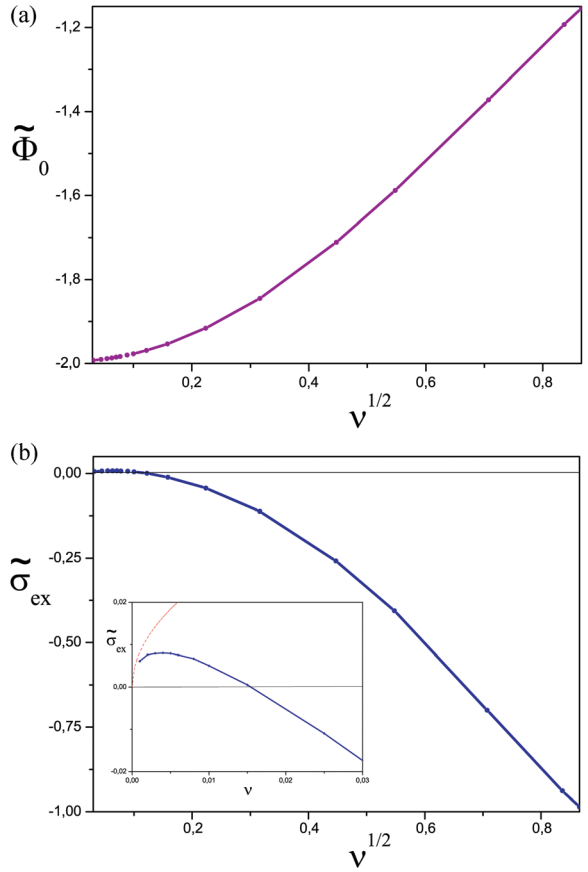

Fig. 4 (a) The surface potential $\tilde{\Phi}_0$ as a function of $\sqrt{\nu}$. (b) The excess charge $\tilde{\sigma}_{ex}$ as a function of $\sqrt{\nu}$. Inset: $\tilde{\sigma}_{ex}$ *vs.* ν for $\nu < 0.03$. The dashed line represents the asymptotics for $\nu \ll 1$ according to eqn (20).

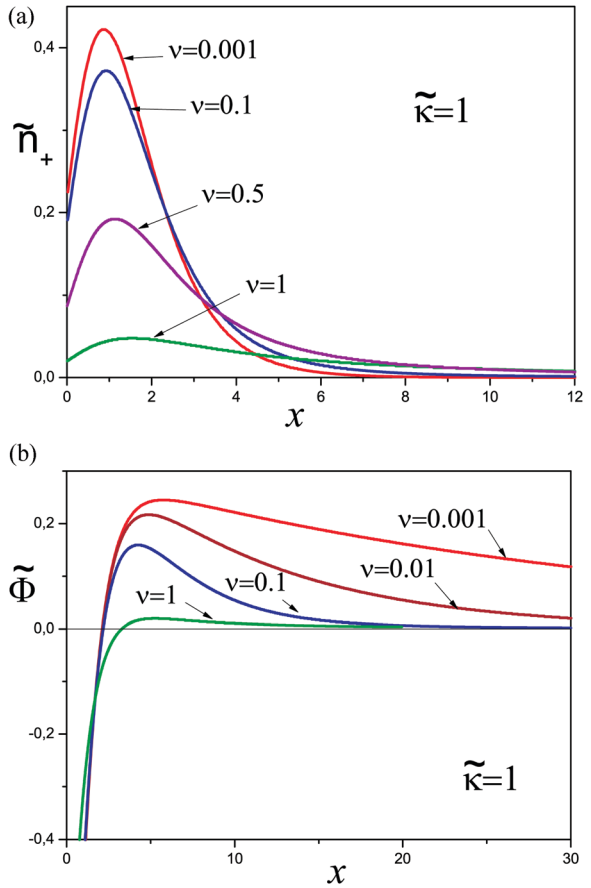

Fig. 5 (a) Concentration profiles of the charged monomers at $\tilde{\kappa} = 1$. (b) The potential profiles at $\tilde{\kappa} = 1$.

$$\frac{d^2\tilde{\Phi}}{dx^2} = -\tilde{\psi}^2 + \nu\tilde{\Phi}, \quad \left.\frac{d\tilde{\Phi}}{dx}\right|_{x=0} = 1, \quad \tilde{\Phi}|_{x=\infty} = 0. \qquad (22)$$

A series of profiles for the concentration of charged monomers and the electric potential are shown in Fig. 5–7 for $\tilde{\kappa} = 1,\ 0,\ -1$ and different values of ν. In all cases the potential passes through a maximum whose height decreases with the ionic strength in the bulk solution, and so does the polymer concentration at $\kappa > 0$. By contrast, the surface potential increases as ν is increased (see Fig. 8a).

For any $\tilde{\kappa} > 0$ the polymer layer is not formed for large enough ionic strength, $\nu \geq \nu_c$; $\nu_c \approx 1.35$ for $\tilde{\kappa} = 1$. This effect occurs because the electrostatic interaction is screened and the polymer/wall repulsion becomes dominant at high ionic strength.

The degree of overcharging increases both with increasing polymer/wall attraction energy and ionic strength, see Fig. 8b. At low ionic strength ($\nu \ll 1$) the excess charge $\tilde{\sigma}_{ex}$ shows the following asymptotic behavior: $\tilde{\sigma}_{ex} \simeq \varepsilon\sqrt{\nu}$ (*cf.* eqn (29)), where ε is a function of $\tilde{\kappa}$ which is shown in Fig. 9.

A detailed analysis of the excess charge and the polymer and electric potential profiles at high ionic strength ($\nu \gg 1$) is presented in Appendix B.

3.3 Effect of excluded-volume interactions

Let us turn to the effect of excluded-volume interactions of polymer segments on their adsorption. Below we consider only the most important case of an indifferent surface ($\tilde{\kappa} = 0$) focusing on the regimes with negligible contribution of one of the virial coefficients: $\tilde{C} = 0$ or $\tilde{B} = 0$.

We start with the case $\tilde{C} = 0$, $\tilde{B} \neq 0$. In Fig. 10 the density of polymer charge and potential profiles are shown. The adsorbed layer thickens with increasing attraction between the monomers or ionic strength. The excess charge also increases with the ionic strength. The plots of $\tilde{\sigma}_{ex}$ for different values of the second virial parameter are shown in Fig. 11. In the case of attractive interactions between monomers ($\tilde{B} < 0$) the system of eqn (10) and (11) has a well-defined stable solution if $\tilde{B} > \tilde{B}_c(\nu)$. For salt free conditions, the critical value of the second virial parameter is $\tilde{B}_c \approx -2.15$ (for $\nu = 0$). The excess charge monotonically decreases while B is passing from poor to good solvent conditions, and so does the reduced eigenvalue ε (*cf.* Fig. 12). At high ionic strength, $\nu \gg 1$, the critical excluded volume parameter is $\tilde{B}_c \simeq -1/\nu$ (*cf.* Appendix B and eqn (A3)).

Finally we address the effect of three-body interactions, $\tilde{C} > 0$. The profiles of $\tilde{n}_+(x)$ and $\tilde{\Phi}(x)$ obtained in this case using eqn (10) and (11) are shown in Fig. 13a–d. The dependence of the excess charge on the ionic strength is shown in Fig. 14.

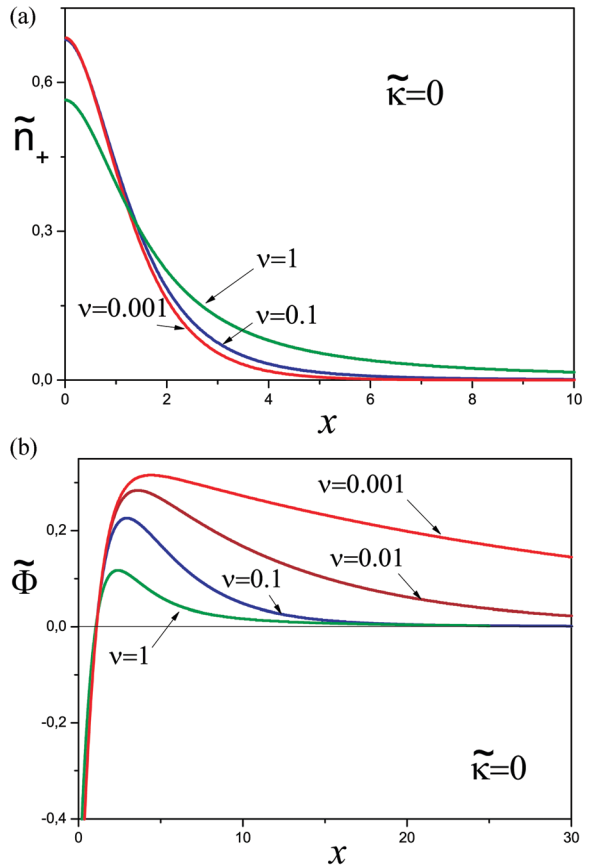

Fig. 6 (a) Concentration profiles of charged monomers for $\tilde{\kappa} = 0$. (b) The potential profiles at $\tilde{\kappa} = 0$.

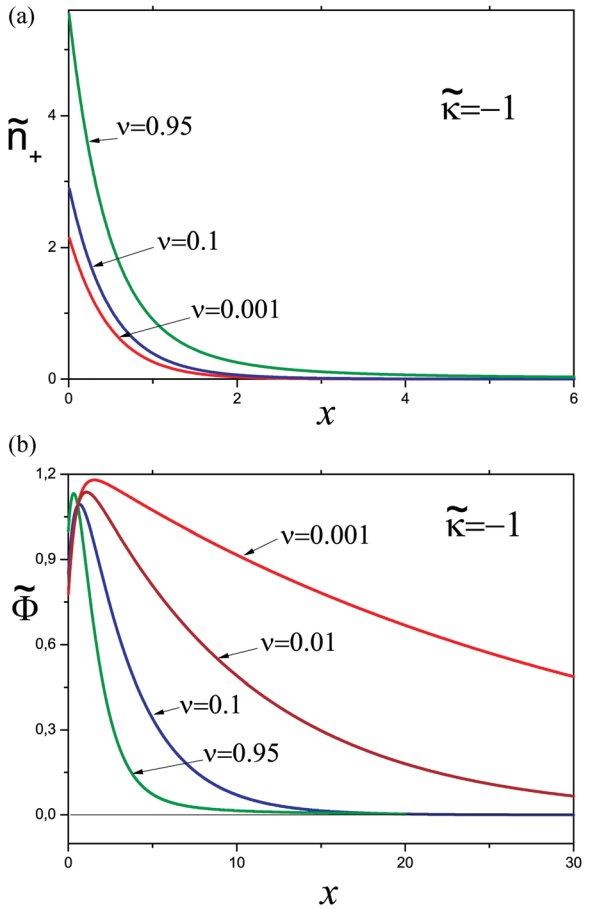

Fig. 7 (a) Concentration profiles of charged monomers at $\tilde{\kappa} = -1$. (b) The potential profiles at $\tilde{\kappa} = -1$.

The degree of overcharging decreases as the third virial coefficient is increased; $\tilde{\sigma}_{ex}$ also decreases at high ionic strength for $\tilde{C} \gtrsim 0.5$.

The reduced thickness $\tilde{h} = h/h_0$ of the adsorbed layer is plotted in Fig. 15a as a function of the third virial parameter $\tilde{C}$ for the salt free case; $\tilde{h}$ increases with $\tilde{C}$ in accordance with analytical results (*cf.* Appendix C). The reduced eigenvalue ε (*cf.* Fig. 15b) monotonically decreases with $\tilde{C}$ reflecting the similar behavior of σ_{ex}.

4 Summary of the main results and discussion

4.1 The region of validity and essential variables

In this paper we considered the equilibrium structure of PE layers adsorbed on oppositely charged surfaces. The study concerns weakly charged PE chains, $f \ll 1$, with very low bulk concentration (dilute solution). The weak charge condition is very important: it allows us to focus on the mean-field solution regime, where the existing well-established theoretical frameworks can be harnessed to cast quantitative results. In Appendix A we specify two main conditions of applicability of the mean-field approach demanding that concentration blobs are Gaussian (eqn (A1)) and electrostatic potential is low (eqn (A2)). It is only for $f \ll 1$ that the two conditions are compatible defining a wide range of eligible surface charge densities (σ). Note that the second condition also ensures that electrostatic screening effects can be described by the mean field model ($r_D \gg \ell_B$): in fact, the relevant length-scale defining the characteristic Debye length r_D is the adsorbed layer thickness h_0 (*cf.* eqn (9)), which is much longer than $a/\sqrt{f}$ by virtue of eqn (9) and (A2), hence $r_D \gg a/\sqrt{f} \gg \ell_B$.

One focus of our study concerns charge inversion and the dependence of the excess charge $e\sigma_{ex}$ (that is, the total charge of the surface and adsorbed polymer) and of the layer thickness h on various parameters: bare surface charge $e\sigma$, ionic strength c_b, fraction of charged units f, short-range specific attraction of the polymer backbone to the surface (its magnitude is characterized by the parameter κ), and virial parameters B and C. We quantitatively described (both numerically and analytically) the effect of monomer interactions considering both the regime where binary interactions (B) are dominating and the Θ-regime with significant 3-body interactions (C).

Both σ_{ex} and h are generally related to the polymer adsorbance

$$\Gamma = \int_0^\infty n(z)\mathrm{d}z \qquad (23)$$

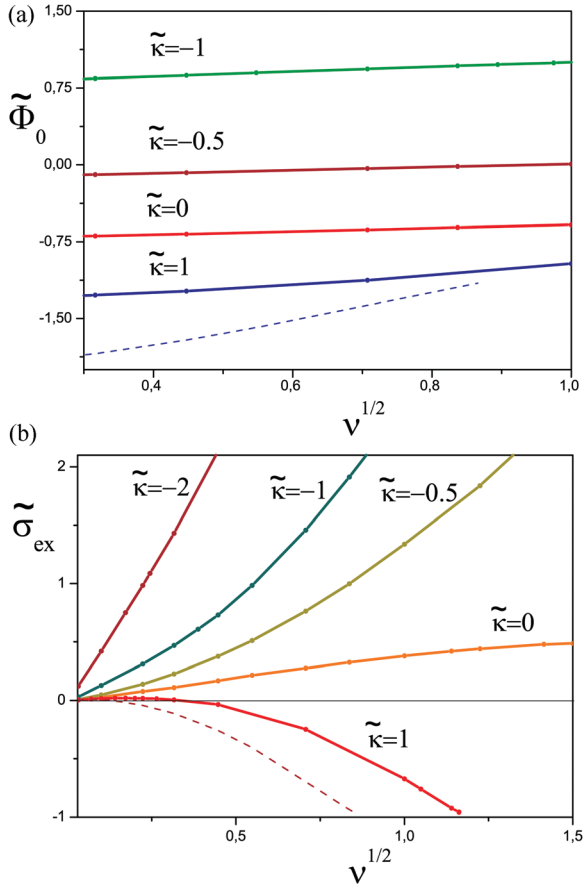

Fig. 8 (a) The surface potential $\tilde{\Phi}_0$ as a function of $\sqrt{\nu}$ for different values of parameter $\tilde{\kappa}$. (b) The excess charge $\tilde{\sigma}_{ex}$ as a function of $\sqrt{\nu}$ for different values of parameter $\tilde{\kappa}$. Dashed lines correspond to the case of the repulsive hard wall ($\kappa \to \infty$).

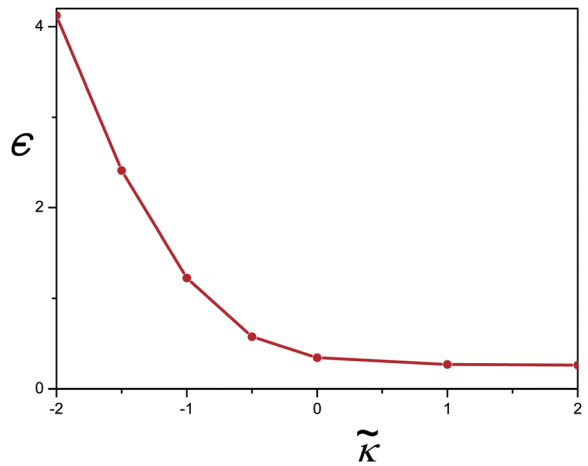

Fig. 9 The reduced eigenvalue ε as a function of $\tilde{\kappa}$.

where $n(z)$ is the concentration of PE monomers at distance z from the surface and $n_{max} = \max n(z)$:

$$\sigma_{ex} = f\Gamma - \sigma, \quad h = \Gamma/n_{max}. \tag{24}$$

The characteristic thickness of the adsorbed layer $h_0 = \left(\frac{a^2}{\sigma f \tilde{\ell}_B}\right)^{1/3}$ (*cf.* eqn (9)) serves as a natural length-scale for the adsorption structure. Using this length we identified the following essential reduced parameters corresponding to the ionic strength, the monomer/surface and excluded-volume interactions: $\nu = h_0^2/r_D^2 = 2\tilde{\ell}_B^{1/3} a^{4/3} (\sigma f)^{-2/3} c_b$, $\tilde{\kappa} = \kappa h_0$, $\tilde{B} = B/B_0$, $\tilde{C}/C_0$, where

$$B_0 = \frac{a^2 f}{\sigma h_0}, \quad C_0 = 2\left(\frac{af}{\sigma}\right)^2 \tag{25}$$

are the characteristic values of the second and the third virial parameters of non-electrostatic monomer interactions. This way we minimize the number of variables to deal with and obtain universal predictions for the adsorbed layer structure in terms of this minimal set of reduced parameters.

In addition to the Debye–Hückel (DH) approximation for monovalent ions (weak charge, $\Phi \ll 1$), we use the ground-state dominance (GSD) approximation to describe the chain statistics. The latter approximation is fully justified for very long (infinite) polymer chains considered in the present paper. In practice the chains are finite, and the GSD approximation is valid for $N \gg N^*$, where $N^* \sim h^2/a^2$ is defined by the condition $R_{coil} = aN^{1/2} \gg h$,[14,16] meaning that the coil size (Gaussian gyration radius) R_{coil} must well exceed the characteristic adsorbed layer thickness h. For example, $h = h_0$ in the simplest case of no added salt, no specific monomer-wall attraction and no excluded-volume interactions, so the GSD condition then becomes[7]

$$N \gg \left(\sigma f \tilde{\ell}_B a\right)^{-2/3}.$$

The same GSD condition ($N \gg N^*$) also ensures that the concentration of PE segments in the adsorbed layer, $n \sim n_{max}$, can be significant (say, semidilute) even if the bulk concentration n_b is very small (very dilute bulk polymer solution as considered in the present paper). For example, in the case of no added salt the condition $n_b/n_{max} \ll 1$ can be formally provided if $N|E_0| \gg 1$ which is equivalent to $N \gg N^*$.

It is also worth noting that the regime $R_{coil} \gg h$ is the most typical for high polymers: in the opposite case $R_{coil} \ll h$ the polymer coils can be considered similarly to small multi-valent ions. In the latter regime ($N \ll N^*$) the PE chains are attracted less strongly to the substrate, so the adsorbance Γ typically decreases for shorter chains. The dependence of the PE adsorption profiles on the chain length (N) was analyzed in ref. 9 using the self-consistent field theory. The N-effect saturates for long chains in reasonable agreement with the theoretical criterion $N \gg N^*$ considered above.

4.2 The ground-state eigenvalue and the low-salt limit

The adsorbed layer structure (including the polymer profile $n(z)$) is defined by eqn (3) and (4) which involve a free parameter, the eigenvalue E. Below we discuss the general analytical results showing how E is related to the excess charge in the regime of low salt, $r_D \gg h$. There is an important formal distinction between the case of no salt ($c_b \propto \nu = 0$) and any finite ionic strength ($\nu > 0$): as demonstrated below the

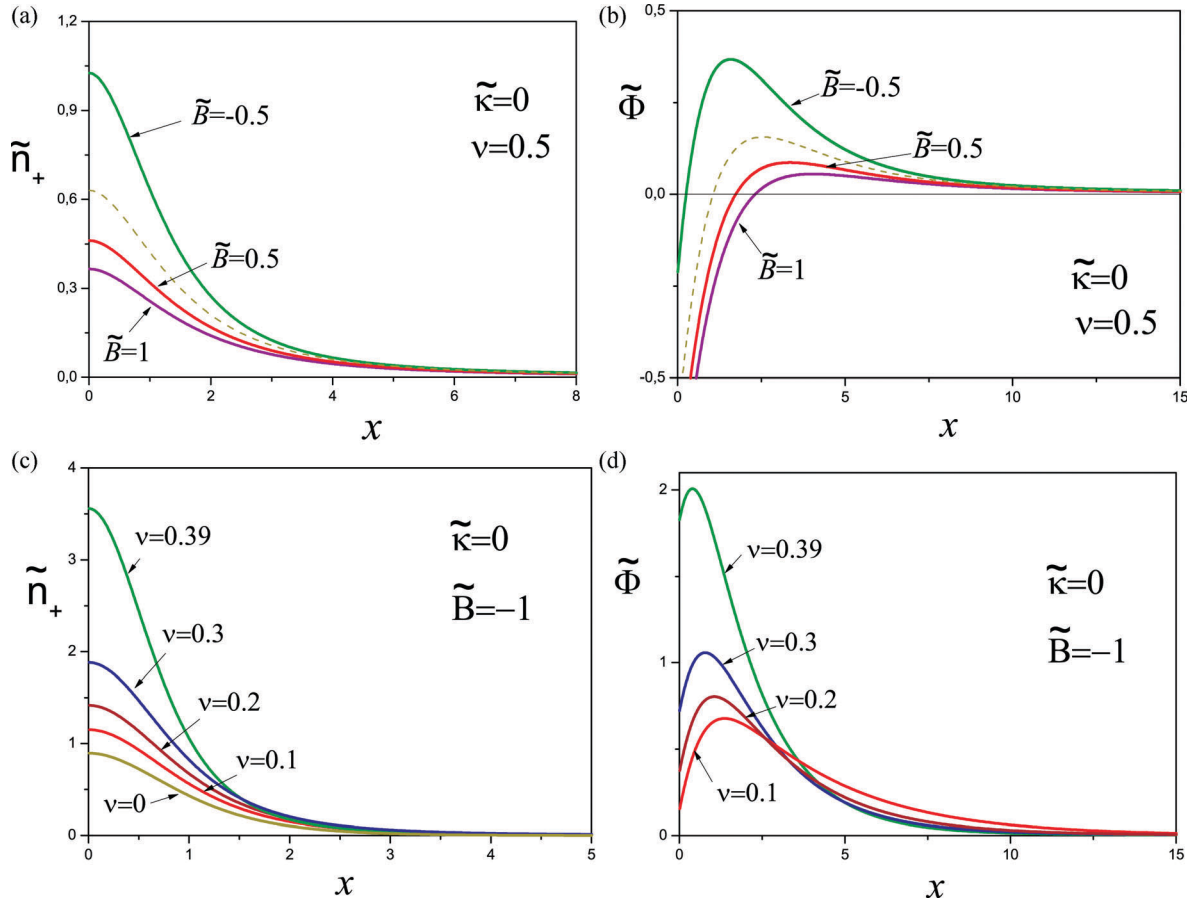

Fig. 10 (a) Concentration profiles of charged monomers for different values of the second virial parameter $\tilde{B}$ and ν = 0.5. (b) Potential profiles for different values of $\tilde{B}$ and ν = 0.5. (c) Concentration profiles of charged monomers for different values of ionic strength ν and $\tilde{B}$ = −1. (d) Potential profiles for different values of ν and $\tilde{B}$ = −1. Dashed lines always correspond to $\tilde{B}$ = 0.

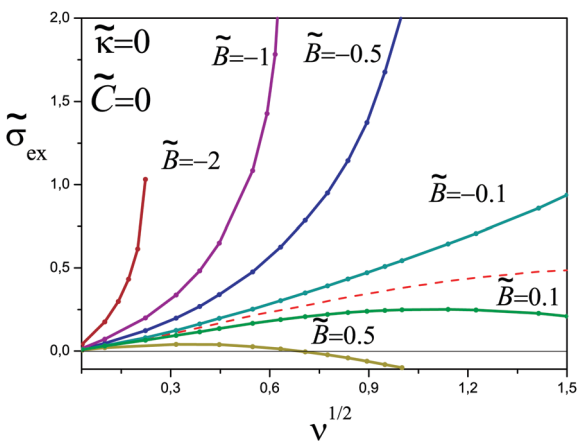

Fig. 11 The excess charge as a function of $\sqrt{\nu}$ for different values of the second virial parameter $\tilde{B}$ and $\tilde{C}$ = 0. The dashed line corresponds to $\tilde{B}$ = 0.

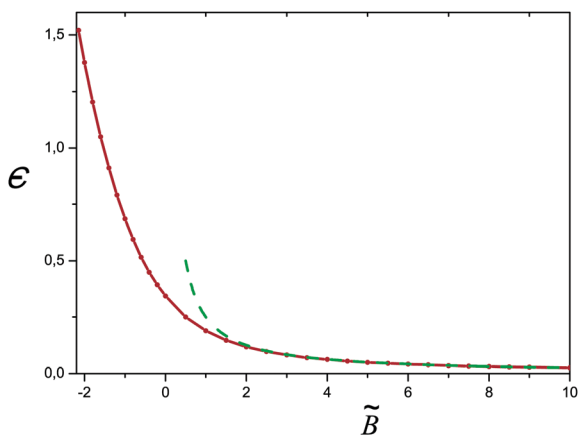

Fig. 12 The reduced eigenvalue ε for the salt free case (ν = 0) as a function of $\tilde{B} = B/B_0$. The dashed curve shows the theoretical asymptotics according to eqn (C6).

ground-state eigenvalue E is negative in the former case, while E = 0 otherwise.

For $\nu > 0$, the free energy F of the adsorbed layer can be considered as a function of adsorbed amount Γ: $F = F(\Gamma)$. The total free energy of the system (layer + bulk solution) is $F(\Gamma) - \mu_b\Gamma$ + const, where μ_b is the monomer chemical potential in the bulk solution (*cf.* eqn (1)):

$$\mu_b = \frac{k_B T}{N}\ln(n_b) + \mu_{ex}(n_b).$$

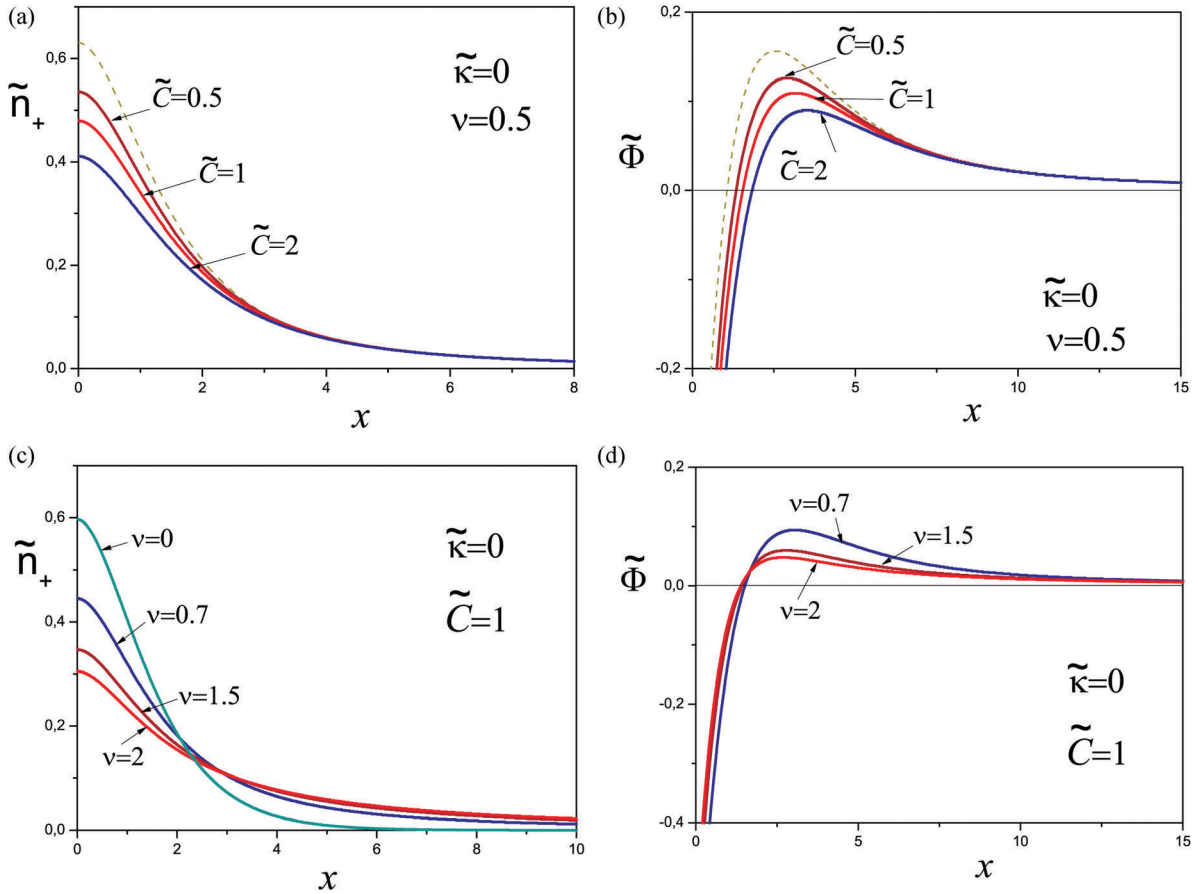

Fig. 13 (a) Concentration profiles of charged monomers for $\nu = 0.5$, $\kappa = 0$, $B = 0$ and different values of the third virial parameter $\tilde{C}$. (b) Potential profiles for different values of $\tilde{C}$. (c) Concentration profiles of charged monomers for different values of ionic strength (ν) and $\tilde{C} = 1$. (d) Potential profiles for different values of ν and $\tilde{C} = 1$. Dashed lines correspond to $\tilde{C} = 0$, $\nu = 0.5$.

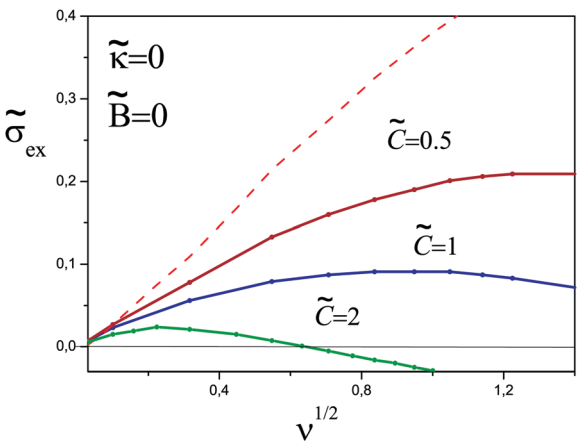

Fig. 14 The excess charge as a function of $\sqrt{\nu}$ for different values of the third virial parameter. The dashed line corresponds to $\tilde{C} = 0$.

The electrostatic potential is not involved in μ_b since it vanishes in the bulk by definition: $\varphi \to 0$ at $z \to \infty$. The first ideal-gas term in the above equation also vanishes since $N \to \infty$, and so does the second term (*cf.* eqn (1)) in the dilute limit $n_b \to 0$, hence $\mu_b = 0$.

The adsorbed layer is formed since the total free energy $F(\Gamma) - \mu_b\Gamma$ decreases with Γ at low Γ. The equilibrium state (saturated adsorbed layer) corresponds to the minimum of the total free energy, *i.e.*

$$\frac{\partial F}{\partial \Gamma} = \mu_b = 0.$$

Considering F as a functional of concentration profile, $F = F[n(z)]$, we arrive at the general minimization condition

$$\frac{\delta F[n]}{\delta n(z)} = 0. \qquad (26)$$

Recalling that $F = F_{conf} + F_{int}$, where F_{conf} is the square-gradient conformational free energy and F_{int} is the free energy of all interactions (including F_{ex} and electrostatic contributions), one can see that eqn (26) is equivalent to the Edwards equation (eqn (4)) with $E = 0$.‡

The situation for no salt ($\nu = 0$) is different: here, $F[n]$ is defined only for $\Gamma = \sigma/f$: F is infinite for any other Γ due to violation of the electroneutrality. Therefore $F[n]$ has to be minimized under the side condition

$$\int_0^\infty n(z)\mathrm{d}z = \sigma/f$$

‡ The result $E = 0$ is strictly valid only for $N \to \infty$. For finite chains it is replaced by $E \simeq -(1/N)\ln(n_{max}/n_b)$.[31]

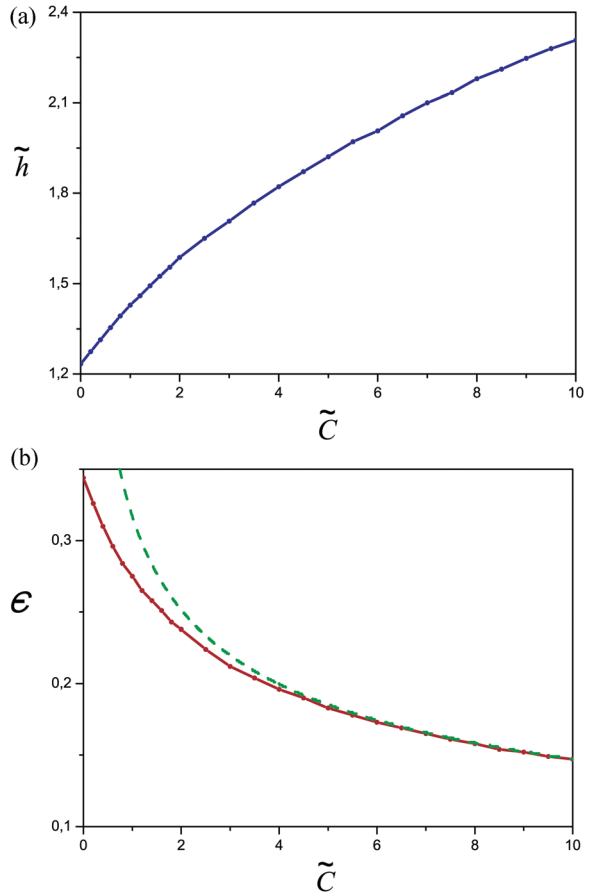

Fig. 15 (a) The reduced thickness of the adsorbed layer $\tilde{h}$ (defined by the condition $\tilde{n}(\tilde{h}) = 0.5\tilde{n}(0)$) as a function of $\tilde{C} = C/C_0$ in the salt free case ($\nu = 0$). (b) The reduced eigenvalue ε as a function of $\tilde{C}$. The dashed curve shows the theoretical asymptotics according to eqn (C9).

formally leading to the variational equation

$$\frac{\delta F[n]}{\delta n(z)} = \lambda$$

(where λ is the Lagrange multilayer) and thus giving rise to Edwards equation (eqn (4)) with $E = \lambda/(k_BT) \neq 0$. The above equation formally implies that

$$\frac{1}{k_BT}\frac{\partial F}{\partial \Gamma} = E \text{ at } \Gamma = \sigma/f, \quad \nu = 0. \tag{27}$$

The following corollary can be deduced from the previous point: obviously Γ must tend to σ/f at $\nu \to 0$, that is, Γ is continuous at $\nu = 0$, and so is the whole polymer profile $n(z)$. By virtue of the Edwards equation (eqn (4)), the same statement applies to $U(z) - E$ and $f\Phi(z) - E$, where $\Phi = e\varphi/(k_BT)$. Hence $\lim_{\nu\to 0}[f\Phi(z)] = f\Phi_0(z) - E_0$, where subscript '0' corresponds to $\nu = 0$. Recalling also that $\Phi_0(z) \to 0$ at $z \gg h_0$, we find $\lim_{\nu\to 0}\Phi(z) \simeq -E_0/f$ for $z \gg h_0$. In terms of reduced variables this gives $\lim_{\nu\to 0}\tilde{\Phi}(x) \simeq \varepsilon$ for $x \gg 1$, where $\varepsilon = -{h_0}^2E_0/a^2$, $\tilde{\Phi} = \varphi/\varphi_0$, $\varphi_0 = (k_BT/e)\sigma\tilde{\ell}_Bh_0$. Using eqn (11) and taking into account that $\tilde{\psi}(x) \to 0$ for $x \gg 1$ we find the asymptotic behavior of the electrostatic potential at low salt concentrations:

$$\tilde{\Phi}(x) \simeq \varepsilon\exp\left(-\sqrt{\nu}x\right), \quad \nu \ll 1, \quad x \gg 1 \tag{28}$$

On using eqn (19) this leads to the asymptotic equation defining the excess surface charge:

$$\sigma_{ex}/\sigma \simeq \varepsilon\sqrt{\nu}, \quad \nu \ll 1. \tag{29}$$

The above result can also be rationalized in the following way: eqn (27) shows that $\partial F/\partial\Gamma = -k_BT(a/h_0)^2\varepsilon$ is negative at $\Gamma = \Gamma_0 \equiv \sigma/f$ corresponding to exact charge compensation. Therefore, an increase of PE adsorbance ($\Gamma > \Gamma_0$ leading to $\sigma_{ex} = f(\Gamma - \Gamma_0) > 0$) is favorable: $F \simeq \text{const} - k_BT(a/h_0)^2\varepsilon\sigma_{ex}/f$ for small σ_{ex}. The energy penalty ΔF_{es} to pay for this excess charge comes from the long-range electric field generated by σ_{ex} at $z \sim r_D \gg h_0$. Within the DH approximation its energy is $\Delta F_{es} \simeq \frac{k_BT}{2}\tilde{\ell}_Br_D{\sigma_{ex}}^2$. Minimization of $F + \Delta F_{es}$ then gives $\sigma_{ex} \simeq \sigma\varepsilon h_0/r_D$, which is equivalent to eqn (29).

The reduced eigenvalue ε also defines the polymer density profile $\tilde{n}(x) = \tilde{\psi}(x)^2$ in the low salt regime. In the case of no salt ($\nu = 0$) we find that $\tilde{n}(x)$ decays exponentially at large distances:

$$\tilde{n} \sim \exp\left(-2\sqrt{\varepsilon}x\right), \quad x \gg 1.$$

At finite but low ionic strength ($\nu \ll 1$) the asymptotic behavior of $\tilde{n}(x) = \tilde{\psi}(x)^2$ can be obtained using eqn (17) with $\tilde{E} = 0$ and $\tilde{\Phi}(x)$ defined in eqn (28):

$$\tilde{n} \sim \exp\left(-\frac{4\sqrt{\varepsilon}}{\sqrt{\nu}}\left(1 - e^{-\sqrt{\nu}x/2}\right)\right), \quad x \gg 1.$$

Thus, $\tilde{n}$ decays exponentially for $1 \ll x \ll 1/\sqrt{\nu}$ (*i.e.*, for the range $h_0 \ll z \ll r_D$ of real distances z to the surface), and then saturates at a very low level:

$$\tilde{n} \sim e^{-4\sqrt{\varepsilon}/\sqrt{\nu}}, \quad x \gg 1/\sqrt{\nu}.$$

The saturation plateau stays until exponentially long distances, for $x \ll e^{2\sqrt{\varepsilon}/\sqrt{\nu}}$, and it is followed by a power-law decay at even larger distances.

4.3 The Θ-solvent regime: ionic strength and specific polymer/surface interaction effects

For sterically repulsive surfaces and negligible excluded-volume interactions ($B = C = 0$), the only essential parameter is $\nu = {h_0}^2/{r_D}^2$. In this case the low-salt asymptotics, eqn (20), is applicable only for very low $\nu < 10^{-3}$. The excess charge $e\sigma_{ex}$ is positive for $\nu < 0.015$, but its value does not exceed 1% of the surface charge: $\sigma_{ex}/\sigma < 1\%$. For $\nu > 0.015$, the adsorbed layer enters the charge undercompensation regime ($\sigma_{ex} < 0$), and the PE charge disappears completely ($\sigma_{ex} = -\sigma$) at $\nu = \nu_c \approx 0.78$. The PE layer is not formed at all for $\nu > \nu_c$. The adsorbed layer thickness stays nearly the same, $h \sim h_0$ at $0 < \nu < 0.6$: it is the layer concentration that decreases significantly with ν in this regime. Closer to ν_c the adsorbed layer is characterized by 2 length scales: h_0 (for the proximal region where $n(z)$ is increasing) and h (the layer thickness), the latter is diverging at ν_c.

Note that the ionic strength for the adsorption cutoff, $(c_b)_c = 0.5\nu_c\tilde{\ell}_B^{-1/3}a^{-4/3}(\sigma f)^{2/3}$, is proportional to $(\sigma f)^{2/3}$, so the cutoff ionic strength increases with the polymer charge density (f) in agreement with experimental data.[23]

It is remarkable that the adsorption criterion $\nu < \nu_c$ can be rewritten as

$$r_D{}^3\sigma f\ell_B/a_s{}^2 > \text{const}$$

with const $\approx$ 0.019. The above condition agrees with the criterion for single chain adsorption transition predicted by Muthukumar.[24]

The revealed significant decrease of PE adsorbance Γ and of the excess PE charge σ_{ex} with addition of salt (beyond a very low threshold, $\nu > 0.004$, corresponding to $r_D < 16h_0$) is in agreement with the numerical results of ref. 8. We also agree with ref. 8 on the very low degree of overcharging in the case of strongly repulsive surfaces. However, our results do not confirm the linear scaling of σ_{ex} with the bare surface charge σ stated in ref. 8 for the electrostatically dominated regime. Rather, we analytically predict $\sigma_{ex} \propto \sigma^{2/3}$ at very low ionic strength ($r_D > 20h_0$) in agreement with our numerical results and with the scaling result of ref. 7.

At the scaling level our results for the layer thickness and the amount of adsorbed polymer for $\nu \ll 1$, $h \sim h_0 \sim \left(\frac{a^2}{\sigma f\tilde{\ell}_B}\right)^{1/3}$ and $\Gamma \sim \sigma/f$, are in agreement with the scaling eqn (11) and (13) of ref. 6 (note their notations $p = f$, $D \sim h$ and the reduced surface potential $|y_s| \sim \sigma h\ell_B$). On the other hand, the results of ref. 6 in the high salt limit contradict our prediction of no adsorption for $\nu > \nu_c$ in the case of sterically repulsive surface (we believe that the origin of this discrepancy lies in the approximate nature of the second term in their eqn (14) which seems to be reasonable for an indifferent rather than for a repulsive surface).

Following Joanny[7] we distinguish the important regime of an indifferent surface where short-range attractive and repulsive interactions of PE segments with the surface are balanced ($\kappa = 0$). In this case the relative excess charge $\tilde{\sigma}_{ex} = \sigma_{ex}/\sigma$ always increases with ionic strength (ν), see Fig. 8b. We identified analytically the following asymptotic behaviors of the excess charge (*cf.* Appendix B):

$$\sigma_{ex}/\sigma \simeq 0.344\sqrt{\nu}, \quad \nu \ll 1; \quad \sigma_{ex}/\sigma \simeq 1 - 3\nu^{-3/2}, \quad \nu \gg 1$$

based on eqn (29) with $\varepsilon \approx 0.344$ and eqn (B4). Interpolating the two asymptotics using Padé approximation (with variable $\sqrt{\nu}$) we find the full dependence on ν:

$$\sigma_{ex}/\sigma \approx \left(1 + \frac{1}{\sqrt{\nu}(0.344 + \nu/3)}\right)^{-1}. \qquad (30)$$

The above equation is in good agreement with numerical results in the whole range $0 \le \nu < \infty$ (*cf.* Fig. 16). It shows that the full charge compensation is attained in the limit of very high ionic strength ($\sigma_{ex}/\sigma \to 1$ at $\nu \to \infty$) in agreement with predictions of ref. 7. On the other hand, σ_{ex} is well below the bare surface charge at $\nu \lesssim 5$ (charge inversion is partial) and σ_{ex} always

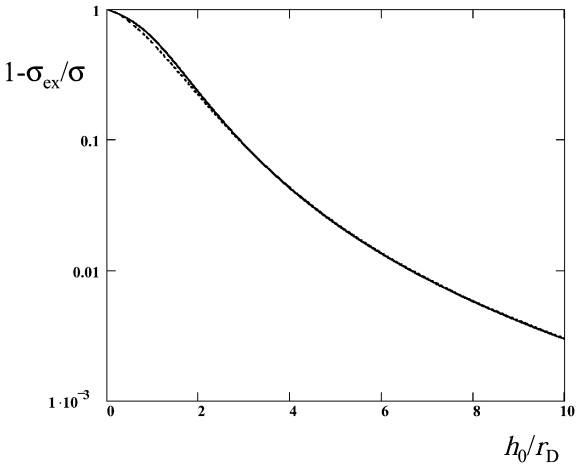

Fig. 16 The dependence of $1 - \tilde{\sigma}_{ex}$ *vs.* $\sqrt{\nu}$ for an indifferent surface ($\kappa = 0$): analytical interpolation, eqn (30) (solid line); numerical results based on eqn (21), (22) and (19) (dashed line).

monotonically increases with ν for $\kappa = 0$. In particular, the excess charge significantly increases with salt concentration in the intermediate range of ionic strength, $10 \gtrsim \nu \gtrsim 0.1$. This result is in accord with numerical data for ref. 8 pointing to moderate σ_{ex}/σ for nearly indifferent surfaces (incomplete charge inversion).

Returning to the scaling level in the high salt regime ($\nu \gg 1$), our results for the layer thickness and the total polymer adsorbance, $h \simeq \nu h_0 \sim a^2/(\sigma f\tilde{\ell}_B r_D{}^2)$ and $\Gamma = (\sigma + \sigma_{ex})/f \sim 2\sigma/f$ (*cf.* Appendix B, eqn (B3) and (B4)), are consistent with eqn (15) and (17) of ref. 6.

The effect of polymer/surface interactions (κ) can be gathered from Fig. 8b: surface repulsion suppresses PE adsorption, leading to a smaller or negative σ_{ex}, and a somewhat thicker but more dilute adsorbed layer. Quite naturally, attractive surface ($\kappa < 0$) enhances PE adsorption, so the adsorbed layer becomes thinner and denser in this regime. These conclusions are backed by our analytical results described below (*cf.* Appendix B): in the high salt regime, $\nu \gg 1$ (*i.e.* $r_D \ll h_0$), the layer is characterized by 2 length-scales: short, the Debye screening length r_D, and long, $D \sim D_0 \equiv h_0{}^3/r_D{}^2$ defining the layer thickness $h \simeq D$. The effective extrapolation length D is defined more precisely in eqn (B5) (note that $\tilde{D} = D/h_0$):

$$\frac{1}{D} \simeq \frac{1 - 1.5\nu^{-1.5}}{D_0} - \kappa\left(1 - 2\nu^{-1.5}\right). \qquad (31)$$

It shows that D diverges at $\kappa D_0 \simeq 1 + 0.5\nu^{-1.5}$; for larger κD_0 the PE layer is not formed. For $\kappa < 0$ and $|\kappa|D_0 \gg 1$, the layer thickness h decreases as $h \simeq D \sim 1/|\kappa|$. While eqn (31) is more precise than the relevant result (eqn (8)) of ref. 7, the two equations fully agree in the limit $\nu \to \infty$ (note that by definition $-\kappa = 1/d$, where d is the surface extrapolation length[7]).

Turning to the excess charge in the high salt regime ($\nu \gg 1$), we find that

$$\sigma_{ex}/\sigma \simeq -1 + 2D_0/D \simeq 1 - 3\nu^{-1.5} - 2\kappa h_0\nu(1 - 2\nu^{-1.5}). \qquad (32)$$

For $1 \gg \kappa h_0 > 0$, the function $\sigma_{ex} = \sigma_{ex}(\nu)$ shows a maximum at a large $\nu = \nu_{max} \simeq (4\kappa h_0/9)^{-0.4}$ with $\max(\sigma_{ex}/\sigma) \simeq 1\text{–}4.61(\kappa h_0)^{0.6}$ corresponding to an incomplete charge inversion. At larger ionic strength, $\nu > \nu_{inv} \simeq 0.5(\kappa h_0)^{-1}$ the excess charge becomes negative entering the charge undercompensation regime. This behavior is in agreement with numerical results of ref. 8 (in the case of 'chemically' repulsive surface). At even higher $\nu > \nu_c \simeq (\kappa h_0)^{-1}$ the adsorbed layer disappears completely ($\sigma_{ex} = -\sigma$). By contrast, in the case of attractive surface ($\kappa = -1/d < 0$) the excess charge always increases with the salt amount (*cf.* Fig. 8b). The full charge inversion is predicted at sufficiently high ionic strength, $\nu > \nu_f \simeq \left(\frac{2}{3}|\kappa|h_0\right)^{-0.4}$ for $|\kappa| \ll 1/h_0$.

At low ionic strength, $\nu \ll 1$, the excess charge is small unless the surface is strongly attractive, $\kappa < 0$, $|\kappa h_0| \gg 1$. In this regime the polymer density profile is nearly exponential, $n(z) \propto \exp(-2z/h)$. The layer thickness and the excess charge are

$$h \simeq 1/|\kappa|, \quad \sigma_{ex}/\sigma \simeq |\kappa|^2 h_0^2 \sqrt{\nu}. \tag{33}$$

The above equation implies that $\sigma_{ex} > \sigma$ for $|\kappa| \frac{1}{h_0}\sqrt{\frac{r_D}{h_0}}$. Thus, the full charge inversion is possible even for $\nu \ll 1$ in the case of specific affinity of PE segments to the surface suggesting that PE multilayers can be stable in the low-salt regime. This conclusion is not in disagreement with experiments.[3,11,17]

4.4 The effect of binary interactions

Qualitatively, the effect of excluded-volume interactions (B) is similar to that of polymer/surface interactions (κ): the excess charge decreases in the marginal solvent conditions ($B > 0$) and increases as the solvent gets poor ($B < 0$) as illustrated in Fig. 11.

The effect of B in the marginal solvent and low salt conditions is analyzed in detail in Appendix C. The main results for $B \gg B_0$ and $\nu \ll B_0/B$ are outlined below: the adsorbed layer structure is characterized by 3 length-scales: $z^* = h_0 x^* = h_0(B_0/B)^{1/4}$, $D = h_0\sqrt{B/B_0}$ and $r_D = h_0/\sqrt{\nu}$. Its effective thickness is $h \simeq D \propto \sqrt{B}$. The polymer density shows significant changes associated with the first two lengths, z^* and D. The electrostatic potential profile $\varphi(z)$ involves the two longer lengths, D and r_D:

$$\varphi(z)/\varphi_0 \simeq -\sqrt{B/B_0}\mathrm{e}^{-z/D} + 0.25(B_0/B)\mathrm{e}^{-z/r_D}$$

where $\varphi_0 = (k_B T/e)\sigma\tilde{\ell}_B h_0$ and $B_0 = h_0^2 f^2 \tilde{\ell}_B$. As in the other weak adsorption regimes, the potential here changes sign being negative at $z \sim D$ and positive at $z \sim r_D \gg D$. The excess surface charge (*cf.* eqn (C7)) is positive and low, $\sigma_{ex} \ll \sigma$:

$$\sigma_{ex} \simeq a^2 f/(4Br_D), \quad B \gg B_0, \nu \ll B_0/B, \quad \kappa h_0 > -0.5B/B_0 \tag{34}$$

and it decreases both with B and r_D. The above equation is based on the asymptotic behavior of the reduced eigenvalue ε established in Appendix C (*cf.* eqn (C6)). Fig. 12 shows that this analytical prediction is in excellent agreement with our numerical results for $B/B_0 \gtrsim 1.5$. Interestingly, both σ_{ex} and $h \simeq D$ are nearly independent of the surface charge σ in this regime:

$$h \simeq \frac{1}{f}\sqrt{\frac{B}{\tilde{\ell}_B}} \equiv h^* \tag{35}$$

As discussed in Appendix C, σ_{ex} and h are also nearly independent of the monomer/surface interactions as long as $\kappa > 0$ or $|\kappa h_0| < 0.5B/B_0$. For strongly attractive surface, $\kappa < 0$, $|\tilde{\kappa}| - \tilde{B}/2 \gg 1/\sqrt{\tilde{B}}$ and $\tilde{B} \gg 1$, we obtain

$$h^{-1} \simeq |\kappa| - \frac{B\sigma}{2a^2 f}, \quad \sigma_{ex} \simeq \frac{a^2}{f\tilde{l}_B}\frac{1}{r_D}\left(|\kappa| - \frac{B}{2a^2 f}\sigma\right)^2, \quad \nu \ll 1. \tag{36}$$

The above equations agree with eqn (33) for $B = 0$. Note that the adsorbed layer thickness h decreases as the monomer/surface attraction gets stronger, but h becomes larger for better solvent quality (larger B) or denser surface charge (higher σ), while the excess charge σ_{ex} shows the opposite tendencies. The polymer density profile in this regime is given in eqn (C5).

In the high salt regime, $\nu \gg 1$, the effect of excluded-volume parameter $\tilde{B}$ is quantitatively equivalent to the effect of monomer/surface interactions ($\tilde{\kappa}$) provided that both parameters are sufficiently small, $\tilde{B} \ll 1/\nu$ and $\tilde{\kappa} \ll 1/\nu$ (*cf.* eqn (B8)). For $\tilde{B} + \tilde{\kappa} > 0$, the excess charge $\tilde{\sigma}_{ex}$ shows a maximum as a function of ionic strength (ν). Such behavior was observed for cationic PEs adsorbed on silica surfaces.[23,25] Conversely, for $\tilde{B} + \tilde{\kappa} < 0$, a monotonic increase of $\tilde{\sigma}_{ex}$ and full charge inversion are predicted at high ν.

To better illustrate the effect of solvent conditions for $\nu \gg 1$ let us consider the case of an indifferent surface ($\kappa = 0$) and $|\tilde{B}| \ll 1$ in more detail. Here the excess charge is (*cf.* eqn (B6)):

$$\tilde{\sigma}_{ex} \simeq -1 + \frac{2}{1 + \tilde{B}\nu}\left(1 - 1.5\nu^{-1.5}\right). \tag{37}$$

In marginal solvent conditions ($B > 0$), an overcompensation of surface charge is predicted for $\nu < \tilde{B}^{-1}(1 - 3\tilde{B}^{3/2}) \equiv \nu_{inv}$. In this range of ionic strength the excess charge first increases and then decreases with ν showing a maximum $\tilde{\sigma}_{ex} \simeq 1 - 4.61\tilde{B}^{3/5}$ at $\nu \simeq (4\tilde{B}/9)^{-2/5}$ corresponding to a partial charge inversion. The surface charge is undercompensated at a larger ionic strength: $\tilde{\sigma}_{ex} < 0$ at $\nu > \nu_{inv}$. This regime is entered as soon as the Debye length becomes short enough, $r_D < h^*$, where the length h^* is defined in eqn (35).

In poor solvent conditions, $B < 0$, the excess charge always increases with ν. A full charge reversal ($\sigma_{ex} > \sigma$) occurs for $\nu > \nu_f$ with

$$\nu_f \simeq \left(\frac{3}{2|\tilde{B}|}\right)^{2/5}. \tag{38}$$

Thus, in a moderately poor solvent the full charge inversion can be easily achieved by increasing ionic strength in the regime $\nu \gg 1$. This conclusion is valid both for indifferent or slightly repulsive surfaces. It is backed by our numerical results (see Fig. 11) and

agrees with the strong charge inversion effect found numerically in poor solvent conditions.[9]

Based on the analytical results for $\tilde{\sigma}_{ex}$ in low and high salt limits (*cf.* eqn (37)) we propose an analytical interpolation (of Padé type with variable $\sqrt{\nu}$) valid for any ionic strength ν (for $\kappa = 0$ and $|\tilde{B}| \ll 1$):

$$\tilde{\sigma}_{ex} \approx \frac{1-\nu\tilde{B}}{1+\nu\tilde{B}}\left[1+\frac{1}{\sqrt{\nu}}\left[0.344+\nu\left(1-\nu\tilde{B}\right)/3\right]^{-1}\right]^{-1}. \qquad (39)$$

The above equation generalizes eqn (30).

4.5 Further remarks

We established that the excess charge in the low-salt regime ($r_D \gg h_0$) is always positive and obeys the general equation (eqn (29)). This result can be compared with the scaling relation

$$\sigma_{ex}/\sigma \sim h/r_D \qquad (40)$$

that was hinted at in ref. 7. The two predictions obviously agree concerning the r_D dependence of σ_{ex}. Moreover, the scaling result of ref. 7 is valid for ideal chains ($B = C = 0$) and repulsive surfaces. However, the two equations imply different dependencies on other parameters. In particular, we found that eqn (40) overestimates σ_{ex} in the case of significant excluded-volume interactions of chain segments. For example, in Θ-solvent conditions with sufficiently high σ (so that $C \gg C_0$) ref. 7 predicts $\sigma_{ex}/\sigma \propto \sigma^{1/3}$, while our result (*cf.* eqn (C10)) implies that $\sigma_{ex}/\sigma \propto 1/\sigma$, *i.e.*, the opposite trend is predicted: a decrease of the reduced excess charged with the bare surface charge. One possible reason for the failure of the scaling relation, eqn 40, is connected with the fact that the adsorbed layer structure is not characterized by a single length scale (h), but rather involves several characteristic lengths in the relevant regimes (see the previous part of the Discussion).

The excess charge σ_{ex} predicted in Appendix C for $C \gg C_0$ at low ionic strength ($\nu \ll 1$) scales as $\sigma_{ex} \propto C^{-1/3}$ (*cf.* eqn (C10)). It is remarkable that the asymptotic analytical equations (eqn (C10) and (C9)) are quantitatively valid for $C/C_0 \gtrsim 4$ as evidenced by the excellent agreement between the numerical and analytical results in this range (*cf.* Fig. 15b).

In this study we considered weakly charged polyelectrolytes with a small fraction f of charged units. One possible realization is a copolymer with neutral units and a small fraction f of charged units. A more common case is a homopolymer with weakly dissociated groups: each unit of the chain can be charged with probability f. Our theory is applicable in both cases. Note that in the latter case the PE charge is not necessarily constant: it depends on the electric potential. However, for weak potentials required by the DH approximation this dependence can be neglected.

The results on charge inversion considered in this paper may provide some basis for understanding the structure of PE multilayers (PEMs),[3,11,12] but we do not claim a direct relevance of the adsorption results to PEMs. For example, the full charge inversion regime does not necessarily imply that PEM formation is mainly driven electrostatically. We believe however that the quantitative model of PE adsorption considered in this paper and the approach taken to analyse it can be usefully applied to study PEM structure. It is a challenging task to quantitatively assess the role of electrostatic interactions in different regimes of PEM formation. We presume that these interactions always contribute to PEM stability. In fact, as was correctly pointed out in ref. 7, even in the regime of charge undercompensation the electrostatic potential outside the last sublayer of PEM is attractive for the new-coming PE chains forming yet another sublayer. We verified that this feature is generally valid in all the regimes.

5 Conclusions

1. The adsorbed PE layer structure and charge compensation effect can be described in terms of the minimal set of the following reduced variables reflecting a self-similar structure of flexible PE chains: $\tilde{h} = h/h_0$, $\tilde{\sigma}_{ex} = \sigma_{ex}/\sigma$, $1/\sqrt{\nu} = r_D/h_0$, $\tilde{\kappa} = \kappa h_0$, $\tilde{B} = B/B_0$, and $\tilde{C} = C/C_0$, where h is the layer thickness, $\sigma_{ex} = f\Gamma - \sigma$ is the excess charge (in units of proton charge e and per unit area), ν is the reduced ion strength, κ is the magnitude of specific short-range monomer/surface repulsion (attraction in the case $\kappa < 0$), $h_0 = \left(\frac{a^2}{\sigma f \tilde{\ell}_B}\right)^{1/3}$ is the characteristic electrostatic thickness, $B_0 = \frac{a^2 f}{\sigma h_0}$, and $C_0 = 2\left(\frac{af}{\sigma}\right)^2$. The reduced parameters depend on the bare surface charge σ: $\nu \propto \sigma^{-2/3}$, $\tilde{\kappa} \propto \sigma^{-1/3}$, $\tilde{B} \propto \sigma^{2/3}$, and $\tilde{C} \propto \sigma^2$.

The following main regimes are distinguished based on the reduced excess charge, $\tilde{\sigma}_{ex}$, of the PE layer: $\tilde{\sigma}_{ex} = -1$, no PE layer is formed (the adsorbed charge $f\Gamma = 0$), $-1 < \tilde{\sigma}_{ex} < 0$ charge undercompensation, $0 < \tilde{\sigma}_{ex} < 1$ partial (incomplete) charge inversion, $\tilde{\sigma}_{ex} = 1$ full charge inversion, and $\tilde{\sigma}_{ex} > 1$ charge inversion with amplification.

2. It is found that in the low salt regime ($r_D \gg h_0$) the PE charge always overcompensates the initial surface charge, and that the excess charge $\tilde{\sigma}_{ex}$ is inversely proportional to r_D. We established the general asymptotic relation $\tilde{\sigma}_{ex} \simeq \varepsilon h_0/r_D$, where ε is the reduced ground-state eigenvalue involved in the Edwards eqn (4), for $\nu = 0$. We calculated ε analytically in a number of important asymptotic regimes (for $\tilde{\kappa} \gg 1$, for $\tilde{B} \gg 1$ and any κ, and for $\tilde{C} \gg 1$) and numerically in intermediate regimes.

For strongly repulsive surfaces we predict the overcharging regime ($\sigma_{ex} > 0$) in a very narrow range of low ionic strength, the degree of overcharging being always very small: $\tilde{\sigma}_{ex} < 0.01$. We also obtained an analytical expression, eqn (B6), for the excess charge in the high salt regime, $\nu \gg 1$, and we quantitatively considered the effect of excluded-volume monomer interactions both in the marginally good and poor solvent regimes. All our analytical and numerical results point to the following general trends: excess charge always increases as the solvent quality decreases (lower or negative B), or as the uncharged surface becomes less repulsive or more attractive for PE segments (lower or negative κ).

3. The dependence of the excess charge on the ionic strength (parameter ν) is more complicated. As is follows from eqn (29)

$\tilde{\sigma}_{ex}$ always increases at low ν. Its further behavior depends on the parameters κ and B:

(i) At $\kappa > 0$ (repulsive surface) and $B > 0$ (marginal solvent) $\tilde{\sigma}_{ex}$ varies with ν in a nonmonotonic way reaching maximum $(\tilde{\sigma}_{ex})_{max}$, $1 > (\tilde{\sigma}_{ex})_{max} > 0$, at some $\nu = \nu_{max}$, then decreasing down to $\tilde{\sigma}_{ex} = -1$ at $\nu = \nu_c$. The adsorbed layer disappears at $\nu > \nu_c$. Such behavior of the PE adsorbance Γ (nonmonotonic dependence of $\Gamma = \sigma(1 + \tilde{\sigma}_{ex})/f$ on the amount of added NaCl followed by adsorption cutoff) has been observed experimentally for cationic PEs on silica surfaces.[23,25] For strongly repulsive surfaces ν_{max} is small, so both the surface coverage Γ and excess charge σ_{ex} mostly decrease with ionic strength (see the dashed curve and the curve for $\tilde{\kappa} = 1$ in Fig. 8b) in agreement with experimental data on adsorption of weakly charged polycations on mica.[26]

(ii) For $\kappa > 0$ and $B < 0$ (poor solvent), σ_{ex} monotonically increases with ν diverging at the bulk stability threshold $\nu \to \nu_{max} \simeq 1/|\tilde{B}|$, if $1 \gg |\tilde{B}| > \tilde{\kappa}$. In the opposite case, $|\tilde{B}| < \tilde{\kappa} \ll 1$, the behavior of $\tilde{\sigma}_{ex}$ is nonmonotonic again like in regime (i).

(iii) For $\kappa < 0$ (attractive surface) and $B < 0$, both the excess charge and surface coverage increase monotonically with ionic strength. Such behavior is typically observed for PEs adsorbed onto oppositely charged surfaces with some nonelectrostatic affinity for the polymer.[27–30]

(iv) Finally, for $\kappa < 0$ and $B > 0$, the excess charge increases, reaches a maximum and then decreases down to a plateau value if $\tilde{B} > |\tilde{\kappa}|$, while $\tilde{\sigma}_{ex}$ monotonically increases up to the plateau at high ionic strength in the opposite case, $\tilde{B} < |\tilde{\kappa}|$.

The predicted tendencies are in agreement with experimental results[22] showing a decrease of polymer adsorbance $\Gamma \propto 1 + \tilde{\sigma}_{ex}$ with ionic strength c_b at a low fraction of charged polymer units ($f = 1\%$) and an increase of Γ with c_b at higher $f = 13\%$ and 30%. (Note that $\tilde{B}/|\tilde{\kappa}| = B\sigma/(\kappa a^2 f) \propto 1/f$, hence a transition from the regime $\tilde{B} > |\tilde{\kappa}|$ to $\tilde{B} < |\tilde{\kappa}|$ is expected as f is increased.)

4. Concerning the effect of surface charge σ on charge inversion, we find that normally the reduced excess charge $\tilde{\sigma}_{ex}$ decreases as σ is increased. This is always true for indifferent or attractive surfaces. However, in the case of repulsive surfaces ($\kappa > 0$) the excess charge can increase with σ at low σ, so $\tilde{\sigma}_{ex}$ can show a maximum as a function of σ. Such behavior in the regime $\tilde{\kappa} \ll 1$, $\nu \gg 1$ is implied in eqn (B8).

5. In Θ-solvent conditions the full (or stronger) charge inversion ($\sigma_{ex} \geq \sigma$) is expected only with some specific attraction of polymer to the surface ($\kappa < 0$, $|\kappa| \geq |\kappa|_f$, where $1/|\kappa| = d$ is the surface extrapolation length). The critical surface attraction parameter $|\kappa|_f$ always decreases with salt addition following the scaling law $|\kappa|_f \propto {r_D}^5$ at high ionic strength ($\nu \gg 1$, $r_D \ll h_0$). More precisely, $|\kappa|_f \simeq 1.5{r_D}^5/{h_0}^6$, and so critical attraction strength increases with bare surface charge: $|\kappa|_f \propto \sigma^2$ for $\nu \gg 1$. In low salt conditions ($\nu \ll 1$, $r_D \gg h_0$) the magnitude of critical attraction increases significantly: $|\kappa|_f \sim \nu^{-1/4}/h_0$. It is shown however (see Section 4.4) that in poor solvent conditions ($B < 0$) the full charge inversion can be achieved even in the case of repulsive surfaces ($\kappa > 0$). This conclusion is in agreement with the numerical results of ref. 9.

6. The surface layer structure is generally characterized by multiple essentially different length-scales including the PE layer mean thickness h (*cf.* eqn (24)) and the Debye length r_D. In the case of low ionic strength (long r_D) and significant excluded-volume interactions ($\tilde{B} \gg 1$ corresponding to high enough surface charge σ) the third length $z^* \sim h_0\tilde{B}^{-1/4}$ emerged ($z^* \ll h \ll r_D$). In Θ-solvent conditions with $\tilde{C} \gg 1$ (this again corresponds to sufficiently high σ) two extra lengths are involved: the proximal decay length $z^* \sim h_0\tilde{C}^{-1/6}$ showing how fast the effect of surface interactions fades off away from the surface, and the distal decay length $\xi \sim h_0\tilde{C}^{1/6}$ characterizing the decrease of polymer density in the region $h < z \lesssim r_D$. The characteristic lengths then form the following sequence: $z^* \ll \xi \ll h \ll r_D$.

We also established (both numerically and analytically) that the adsorbed layer thickness h always increases with ionic strength. This conclusion is in agreement with experimental data.[25–27]

Appendix A: marginal solvent and other conditions

Below we outline the regimes of validity for the main approximations used in the paper.

(1) Gaussian chains and weak fluctuation effects: this approximation effectively means that the relevant chain fragment (of size comparable with the adsorbed layer thickness h) is not swollen by monomer interactions. For $r_D \gg h$ we distinguish electrostatic and excluded-volume contributions to the interactions. Electrostatic interactions do not affect much chain conformations on the length-scales h shorter than the electrostatic blob size[18] $\xi_e \sim \left(\frac{a^4}{f^2\ell_B}\right)^{1/3}$: $h \ll \xi_e$. With $h \sim h_0$, where h_0 is the characteristic thickness (defined in eqn (9)) in the low-salt regime, we thus get

$$\sigma \gg \frac{f}{4\pi a^2}. \tag{A1}$$

As for the excluded-volume interactions, the standard criterion of the marginal solvent regime can be used:[19–21] $n \gg B/{a_s}^6$, where $n \sim \frac{\sigma}{fh}$ is the typical concentration in the layer. With $B \sim B_0 = \frac{a^2 f}{\sigma h_0}$ (corresponding to significant binary monomer interactions) the marginal solvent condition becomes $\sigma \gg f/(6^{3/2}a^2)$ which virtually coincides with condition (A1).

In the high salt regime ($r_D \ll h$) electrostatic interactions are equivalent to excluded volume with $B \sim B_0/\nu$ (where $\nu = {h_0}^2/{r_D}^2$), and the layer thickness is $h \sim h_0\nu$, so the marginal solvent condition ($n \gg B/{a_s}^6$) again reduces to eqn (A1). (Note: for higher $\tilde{B} = B/B_0$, *i.e.* $\tilde{B}\nu \gg 1$, the marginal solvent condition is stronger: $\sigma \gg \frac{f}{6\sqrt{6}a^2}\tilde{B}\nu$.)

(2) The Debye–Hückel (DH) approximation: it is hinged on low electric potential, $\Phi \ll 1$. For $r_D \gg h$ (low salt) $\Phi \sim \sigma\ell_B h_0$, so using eqn (9) we get

$$\sigma \ll \frac{\sqrt{f}}{a\ell_B}. \tag{A2}$$

This condition is compatible with eqn (A1) since $f \ll 1$. The same condition (A2) also ensures that the virial approximation is applicable ($Cn^2 \ll 1$).

(3) In the case of attractive monomer interactions, $B < 0$, the total excluded volume $B_{tot} = B + B_{es}$, where $B_{es} \simeq \ell_B r_D^2 f^2$ is the effective additional excluded volume due to the Coulomb repulsion of charged units. The solution stability then demands that $|B| < B_{es}$, which is equivalent to

$$|\tilde{B}|\nu < 1 \tag{A3}$$

in terms of reduced parameters.

Appendix B: theory of PE adsorption at high ionic strength

Here we consider the adsorption profiles and excess charge for $\nu \gg 1$ at different excluded volumes and surface repulsion parameters, $\tilde{B}$ and $\tilde{\kappa}$. We start with the simplest case $\tilde{B} = 0$, $\tilde{\kappa} = 0$ (ideal backbones, indifferent surface).

In this case reduced eqn (4) and boundary conditions are

$$\tilde{\psi}'' = \tilde{\Phi}\tilde{\psi}, \quad \tilde{\Phi}'' = -\tilde{\psi}^2 + \nu\tilde{\Phi}, \quad x > 0, \tag{B1}$$

$$\tilde{\Phi}' = 1, \quad \tilde{\psi}' = 0 \text{ at } x = 0 \tag{B2}$$

where prime ($'$) means d/dx. The second eqn (B1) can be generally solved (with a given $\tilde{\psi}$) in a standard way yielding (*cf.* eqn (12))

$$\tilde{\Phi}(x) = -\Delta e^{-x/\Delta} + \frac{\Delta}{2}\int_{-\infty}^{\infty} \tilde{\psi}(|y|)^2 e^{-|y-x|/\Delta} dy$$

where $\Delta \equiv 1/\sqrt{\nu} = r_D/h_0$ is the reduced Debye length. The above expression was substituted for $\tilde{\Phi}(x)$ in the first eqn (B1), and the latter equation was solved in a perturbative way (with a small parameter Δ) to yield

$$\tilde{\psi}(x) \simeq \frac{\sqrt{2\nu}}{x + \tilde{D}}, \quad \tilde{\Phi}(x) \simeq -\Delta e^{-x/\Delta} + \frac{2}{\left(x + \tilde{D}\right)^2}$$

where the effective extrapolation length

$$\tilde{D} \simeq \nu\left(1 + \frac{1.5}{\nu^{1.5}}\right) \tag{B3}$$

includes the leading correction (for large ν). The reduced excess charge is:

$$\sigma_{ex}/\sigma = -1 + \int_0^{\infty} \tilde{\psi}(x)^2 dx \simeq 1 - 3\nu^{-3/2}, \tag{B4}$$

(note that $\tilde{\sigma}_{ex} \equiv \sigma_{ex}/\sigma = -1 + \tilde{\sigma}_p$ and $\tilde{\sigma}_p = \int \tilde{n}(x) dx \equiv \tilde{\Gamma}$ is the reduced charge of the adsorbed PE layer). The first term (=1) is the limiting value obtained by Joanny,[7] and the second term is the main correction. Our analysis shows that other corrections are subdominant ($\sim 1/\nu^3$). This result indicates that $\sigma_{ex}/\sigma < 1$, so full charge inversion does not occur in this regime (charge inversion is incomplete).

The case of arbitrary κ and B can be considered in a similar way. The result is:

$$\tilde{\psi}(x) \simeq \frac{\sqrt{2\nu/(1 + \tilde{B}\nu)}}{x + \tilde{D}}, \quad \tilde{\Phi}(x) \simeq -\Delta e^{-x/\Delta} + \frac{2}{\left(x + \tilde{D}\right)^2}$$

where

$$\tilde{D} \simeq \frac{\nu}{1 - \tilde{\kappa}\nu + 0.5\nu^{-1.5}(4\tilde{\kappa}\nu - 3)} \tag{B5}$$

is the effective extrapolation length. The reduced excess charge is

$$\begin{aligned} \sigma_{ex}/\sigma &\simeq -1 + \frac{2\nu}{1 + \tilde{B}\nu}\frac{1}{\tilde{D}} \\ &\simeq -1 + \frac{2}{1 + \tilde{B}\nu}\left[1 - \tilde{\kappa}\nu + 0.5\nu^{-1.5}(4\tilde{\kappa}\nu - 3)\right]. \end{aligned} \tag{B6}$$

The above equations are valid as long as $1/\tilde{D} > 0$, which is true for $\tilde{\kappa}\nu < 1 + 0.5\nu^{-1.5}$. For larger $\tilde{\kappa}$, the surface is too repulsive and no adsorption layer is formed, hence $\sigma_{ex} = -\sigma$ in this case. In the case of poor solvent, $B < 0$, another restriction, eqn (A3), is applicable.

The full charge inversion ($\sigma_{ex} = \sigma$) is thus predicted for

$$(\tilde{B})_f\nu \simeq -\tilde{\kappa}\nu\left(1 - 2\nu^{-1.5}\right) - 1.5\nu^{-1.5}. \tag{B7}$$

An even stronger charge overcompensation ($\sigma_{ex} > \sigma$) occurs for $\tilde{B} < (\tilde{B})_f$. On the other hand, eqn (B6) points to charge undercompensation ($\sigma_{ex} < 0$) for a large enough excluded volume parameter $\tilde{B}$.

For small interaction parameters $\left(\tilde{\kappa}\nu \ll 1,\ \tilde{B}\nu \ll 1\right)$, eqn (B6) simplifies as

$$\sigma_{ex}/\sigma \simeq 1 - 2\nu(\tilde{\kappa} + \tilde{B}) - 3\nu^{-1.5}. \tag{B8}$$

Appendix C: the effect of excluded-volume interactions in the low salt regime

For $\nu = 0$, the basic equations are

$$\tilde{\psi}'' = (\varepsilon + \tilde{\Phi})\tilde{\psi} + \tilde{B}\tilde{\psi}^3, \quad \tilde{\Phi}'' = -\tilde{\psi}^2 \tag{C1}$$

$$\tilde{\Phi}' = 1, \quad \tilde{\psi}' = \tilde{\kappa}\tilde{\psi} \text{ at } x = 0 \tag{C2}$$

where $\tilde{B} = B/B_0$ is the reduced excluded volume and ε is an important free parameter, the reduced eigenvalue characterizing the fundamentally interesting case of no salt (see Section 4.2 for more details). The effect of B is negligible if $\tilde{B} \ll 1$. Below we consider the opposite regime, $\tilde{B} \gg 1$, where the adsorbed layer structure is defined by electrostatic and excluded-volume interactions. Their balance demands that

$$\tilde{\Phi} = -\tilde{B}\tilde{\psi}^2, \quad \tilde{\Phi}'' = -\tilde{\psi}^2$$

where the first equation is approximate: we neglected the ψ'' and ε terms related to chain entropy in the first eqn (C1). These

equations can be solved using only the first boundary condition (C1); the result is:

$$\tilde{\Phi}(x) = -\sqrt{\tilde{B}}\mathrm{e}^{-x/\sqrt{\tilde{B}}}, \quad \tilde{\psi}(x) = \tilde{B}^{-1/4}\mathrm{e}^{-0.5x/\sqrt{\tilde{B}}}. \qquad \text{(C3)}$$

The reduced monomer concentration is therefore $\tilde{n}(x) = \tilde{B}^{-1/2}\mathrm{e}^{-x/\sqrt{\tilde{B}}}$, so the reduced thickness of the adsorbed layer is

$$\tilde{D} \simeq \sqrt{\tilde{B}}. \qquad \text{(C4)}$$

It is remarkable that eqn (C3) represents the exact solution of the full system (C1) and (C2) for $\tilde{\kappa} = -1\Big/\left(2\sqrt{\tilde{B}}\right) \equiv \kappa^*$ with $\varepsilon = 1/(4\tilde{B}) \equiv \varepsilon^*$. What happens if $\tilde{\kappa} \neq \kappa^*$? In this case a mismatch between the asymptotic solution, eqn (C3), and the actual boundary condition for ψ gives rise to a perturbation of both functions (ψ and Φ) at short distances $x \lesssim 1/\tilde{B}^{1/4} \equiv x^*$. For $\tilde{\kappa} > 0$, and for $\tilde{\kappa} < 0$, $|\tilde{\kappa}| \ll \tilde{B}$, the resultant $\tilde{\psi}(x)$ involves 2 length-scales, x^* and $\tilde{D}$, $x^* \ll \tilde{D}$:

$$\tilde{\psi}(x) \simeq \tilde{B}^{-1/4}\left[\tanh\left(\frac{x + x_0}{\sqrt{2}x^*}\right)\right]^i \mathrm{e}^{-0.5x/\sqrt{\tilde{B}}}$$

where x_0 is defined by the boundary condition (*cf.* the second eqn (C2)), and $i = 1$ for $\kappa > \kappa^*$, $i = -1$ for $\kappa < \kappa^*$. (The effect of κ on the electrostatic potential $\tilde{\Phi}(x)$ is negligible in the specified region of κ.)

For $x \gg x^*$, the effect of the boundary condition $\left(\tilde{\psi}' = \tilde{\kappa}\tilde{\psi}\right)$ becomes exponentially weak, and for that reason ε stays extremely close to ε^*. A more detailed analysis shows that $\varepsilon \simeq \varepsilon^*$ with an exponentially small error ($\ln|\varepsilon - \varepsilon^*| < -2^{3/2}\tilde{B}^{3/4}$ for $\tilde{B} \gg 1$) if $\tilde{\kappa} > -\tilde{B}/2$.

The opposite case $\tilde{\kappa} < -\tilde{B}/2$ corresponds to very strongly attractive surfaces; in this case $\varepsilon \simeq \left(|\tilde{\kappa}| - \tilde{B}/2\right)^2$, $|\tilde{\kappa}| - \tilde{B}/2 \gg 1\Big/\sqrt{\tilde{B}}$. The polymer density profile in this regime is

$$\tilde{n}(z) \simeq \frac{2}{\tilde{B}}\left(|\tilde{\kappa}| - \tilde{B}/2\right)^2 \sinh^{-2}(z/h + \alpha_0) \qquad \text{(C5)}$$

where $\tilde{n} = n/n_0$, $n_0 = \dfrac{\sigma}{h_0 f}$, $\alpha_0 = \dfrac{1}{2}\ln\left(\dfrac{4|\tilde{\kappa}|}{\tilde{B}} - 1\right)$.

Thus, we get the following general result:

$$\varepsilon \simeq 1/(4\tilde{B}), \quad \tilde{B} \gg 1, \quad \tilde{\kappa} > -\tilde{B}/2. \qquad \text{(C6)}$$

The corresponding excess charge in the low salt regime is

$$\sigma_{\mathrm{ex}}/\sigma \simeq \varepsilon\sqrt{\nu} \simeq \sqrt{\nu}/(4\tilde{B}), \quad \tilde{B} \gg 1,\ \nu \ll 1,\ \tilde{\kappa} > -\tilde{B}/2. \quad \text{(C7)}$$

So far we considered the effect of 2-body excluded-volume interactions (B), neglecting 3-body interactions (C) for simplicity. This assumption requires that $Bn \gg Cn^2$. With $n = n_0\tilde{n}$, $B = B_0\tilde{B}$, $n_0 = \dfrac{\sigma}{h_0 f}$, $B_0 = \dfrac{a^2 f}{\sigma h_0}$, and $\tilde{n} \sim \tilde{B}^{-0.5}$ (see eqn (C3) above) this condition for $\tilde{B} \gg 1$ becomes

$$\sigma \ll \frac{fa}{\sqrt{C}}\tilde{B}^{3/4}.$$

The effect of 3-body interactions is analyzed below in the low-salt theta-solvent conditions ($B = 0$). The reduced 3rd virial parameter is $\tilde{C} = C\sigma^2/(2a^2f^2)$. The effect of C is negligible if $\tilde{C} \ll 1$, *i.e.* if

$$\sigma \ll \frac{fa}{\sqrt{C}} = \sigma_{\mathrm{c}}.$$

Let us consider the opposite regime, $\sigma \gg \sigma_{\mathrm{c}}$, where the effect of monomer interactions is strong. The relevant equations for $\nu = 0$ are

$$\tilde{\psi}'' = (\varepsilon + \tilde{\Phi})\tilde{\psi} + \tilde{C}\tilde{\psi}^5, \quad \tilde{\Phi}'' = -\tilde{\psi}^2, \quad \tilde{\Phi}' = 1. \qquad \text{(C8)}$$

We omit the boundary condition for $\tilde{\psi}$ at $x = 0$, since it nearly does not affect either the profiles or the eigenvalue ε, as it follows from our above analysis of the case $\tilde{B} \gg 1$. (The boundary condition $\tilde{\psi}' = \tilde{\kappa}\tilde{\psi}$ reflecting specific polymer/surface interactions generates a perturbation of polymer density on a short length-scale $x^* \sim \tilde{C}^{-1/6}$.)

Using the same sort of approximation as before we arrive at equations

$$\tilde{\Phi} = -\tilde{C}\tilde{n}^2, \quad \tilde{\Phi}'' = -\tilde{n}$$

where $\tilde{n} = \tilde{\psi}^2$. Their solution is

$$\tilde{\Phi}(x) = -\tilde{\Phi}_0(1 - x/\tilde{D})^4, \quad \tilde{n}(x) = \tilde{n}_0(1 - x/\tilde{D})^2$$

where

$$\tilde{\Phi}_0 = \frac{6^{2/3}}{4}\tilde{C}^{1/3}, \quad \tilde{n}_0 = \frac{6^{1/3}}{2}\tilde{C}^{-1/3}, \quad \tilde{D} = 6^{2/3}\tilde{C}^{1/3}.$$

Thus, the polymer concentration profile shows parabolic dependence on x in this case.

Both functions $\tilde{\Phi}(x)$ and $\tilde{n}(x)$ vanish at $x > \tilde{D}$ within the approximation used above. In reality these functions do not vanish completely, but rather are small in this region ($\tilde{\Phi} \ll \tilde{\Phi}_0$, $\tilde{n} \ll \tilde{n}_0$), showing exponential decay:

$$\tilde{n} \propto \tilde{\Phi} \propto \mathrm{e}^{-2\sqrt{\varepsilon}x}, \quad x > \tilde{D}.$$

To obtain the eigenvalue ε one has to analyse the behavior of both functions in a narrow region around $x = \tilde{D}$, for $|x - \tilde{D}| \lesssim \tilde{\xi}$, where $\tilde{\xi} = 1/\sqrt{\varepsilon}$ is the edge decay length. The result is

$$\varepsilon \simeq 0.317/\tilde{C}^{1/3}, \quad \tilde{C} \gg 1 \qquad \text{(C9)}$$

implying that $\tilde{\xi} \sim \tilde{C}^{1/6}$. The corresponding excess charge at low ionic strength is

$$\sigma_{\mathrm{ex}}/\sigma \simeq \varepsilon\sqrt{\nu} \simeq 0.317\nu^{1/2}\tilde{C}^{-1/3}, \quad \tilde{C} \gg 1, \quad \nu \ll 1. \qquad \text{(C10)}$$

Acknowledgements

We acknowledge the partial support from the International Research Training Group (IRTG) ''Soft Matter Science: Concepts for the Design of Functional Materials''.

References

1 D. H. Napper, *Polymer Stabilization of Colloidal Dispersions Academic*, London, 1983.
2 Y. Lvov, G. Decher, H. Haas, H. Möhwald and A. Kalachev, *Physica B*, 1994, **198**, 89.

3 G. Decher, *Science*, 1997, **277**, 1232.
4 R. R. Netz and D. Andelman, *Phys. Rep.*, 2003, **380**, 1–95.
5 U. Voigt, V. Khrenov, K. Tauer, M. Halm, W. Jaeger and R. von Klitzing, *J. Phys.: Condens. Matter*, 2003, **S15**, 213.
6 I. Borukhov, D. Andelman and H. Orland, *Macromolecules*, 1998, **31**, 1665.
7 J.-F. Joanny, *Eur. Phys. J. B*, 1999, **9**, 117.
8 A. Shafir and D. Andelman, *Phys. Rev. E: Stat., Nonlinear, Soft Matter Phys.*, 2004, **70**, 061804.
9 Q. Wang, *Macromolecules*, 2005, **38**, 8911.
10 A. Shafir and D. Andelman, *Eur. Phys. J. E: Soft Matter Biol. Phys.*, 2006, **19**, 155.
11 G. Decher and B. J. Schlenoff, *Multilayer Thin Films. Wiley-VCH*, Weinheim, 2003.
12 J. F. Quinn, A. P. R. Johnston, G. K. Such, A. N. Zelikin and F. Caruso, *Chem. Soc. Rev.*, 2007, **36**(5), 707–718.
13 S. F. Edwards, *Proc. Phys. Soc., London*, 1965, **85**, 613.
14 I. M. Lifshitz, A. Y. Grosberg and A. R. Khokhlov, *Rev. Mod. Phys.*, 1978, **50**, 683.
15 P.-G. de Gennes, *Scaling Concepts in Polymer Physics*, Cornell Univ. Press, Ithaca, 1979.
16 A. Grosberg and A. Khokhlov, *Statistical Physics of Macromolecules*, American Institute of Physics, New York, 1994.
17 K. Tang and N. A. M. Besseling, *Soft Matter*, 2016, **12**, 1032.
18 P.-G. de Gennes, P. Pincus, F. Brochard and R. M. Velasco, *J. Phys.*, 1976, **37**, 1461.
19 A. R. Khokhlov, *Polymer*, 1978, **19**, 1387.
20 D. Schaefer, J. F. Joanny and P. Pincus, *Macromolecules*, 1980, **13**, 1280.
21 A. N. Semenov and A. A. Shvets, *Soft Matter*, 2015, **11**, 8863.
22 G. Durand, F. Lafuma and R. Audebert, *Prog. Colloid Polym. Sci.*, 1988, **76**, 278.
23 N. Hansupalak and M. M. Santore, *Langmuir*, 2003, **19**, 7423.
24 M. Muthukumar, *J. Chem. Phys.*, 1987, **86**, 7230.
25 S. C. Liufu, H. N. Xiao and Y. P. Li, *J. Colloid Interface Sci.*, 2005, **285**, 33.
26 O. J. Rojas, P. M. Claesson, D. Muller and R. D. Neuman, *J. Colloid Interface Sci.*, 1998, **205**, 77.
27 T. Sennerfors, D. Solberg and F. Tiberg, *J. Colloid Interface Sci.*, 2002, **254**, 222.
28 T. Cosgrove, T. M. Obey and B. Vincent, *J. Colloid Interface Sci.*, 1986, **111**, 409.
29 E. Kokofuta and K. Takahashi, *Macromolecules*, 1986, **19**, 351.
30 M. Kawaguchi, H. Kawaguchi and A. Takahashi, *J. Colloid Interface Sci.*, 1988, **124**, 57.
31 A. N. Semenov, J. Bonet-Avalos, A. Johner and J. F. Joanny, *Macromolecules*, 1996, **29**, 2179.